THESIS

THREE-DIMENSIONAL RECONSTRUCTION AND FINITE ELEMENT MODELING OF ANURAN MIDDLE EAR BIOMECHANICS

Submitted by

Rachel C. Fleming

Department of Biology

In partial fulfillment of the requirements

For the Degree of Master of Science

Colorado State University

Fort Collins, Colorado

Fall 2021

Master's Committee:

Advisor: Kim Hoke

Rachel Mueller
Wolfgang Bangerth

ABSTRACT

THREE-DIMENSIONAL GEOMETRIC AND FINITE ELEMENT MODELING OF SOUND TRANSMISSION IN THE ANURAN MIDDLE EAR

The ancestors of modern-day amphibians were the first vertebrates to evolve a middle ear for land-based hearing. Today's amphibians retain a simple and effective middle ear structure similar to those of their ancestors, and the fundamental mechanisms of these ears may reflect those that served as foundations of hearing in terrestrial vertebrates. Understanding amphibian hearing mechanisms can therefore offer insights into the evolution of the more sophisticated hearing we observe in land-dwelling vertebrates today. Although the anatomy of the amphibian middle ear has been thoroughly described, it is not known to what extent various anatomical properties, such as material properties or shape and size of ear structures, influence middle ear movement and sound transduction. To achieve this, I created 3D finite element models of the middle ears of *Rhinella marina* and *Arthroleptis tanneri*, two anuran species with different ear geometry. To create these models, I segmented middle ear parts from the scan, processed them into volumetric FE models, and set up finite element simulations. I subjected both models to harmonic response simulations at a range of frequencies and measured the sensitivity of the model to changes in various parameters to determine their effects on sound transmission. This study presents a hypothesis-generating tool for ear mechanics research and a better understanding of the biomechanics of how variation in the middle ear affects sound transmission. Additionally, this study may inform future work on the fundamental principles of hearing in terrestrial vertebrates.

ACKNOWLEDGEMENTS

First and foremost, I would like to express my deepest appreciation to my advisor, Dr. Kim Hoke, for your unwavering support and adaptability throughout my three years at CSU. Your valuable advice and suggestions were vital for my growth every step of the way. Thanks also for providing me with opportunities to try several different projects during my master's, and for your patience as I discovered my niche within evolutionary biology. I'm not sure I would've found my passion for vertebrate morphology and biomechanics so early in my career if not for your flexibility and encouragement to try new things. Thanks also for fostering a strong sense of community and belonging in the department and in your lab.

Second, I would like to give thanks to other members of Hoke lab, including Dr. Kim Dolphin, Miles Whedbee, Nathan Phipps, Dr. Laura Stein, Leorah McGinnis, and Amir Alayoubi, for your friendship, helpful ideas, and constructive feedback. Thanks Nathan for being my accountability buddy as we were finishing our theses. I would also like to give a very special thanks to former lab member Dr. Molly Womack, who gave me incredibly useful advice and whose frog ear expertise helped me through various stages of this project. Thanks also to former undergraduates, including Emily Sikora, Jesse Espinoza, and Stephanie McMahon, for your hard work and dedication to your projects, I'm rooting for you as you continue in your careers!

Third, I would like to extend my sincere thanks to my committee members Dr. Wolfgang Bangerth and Dr. Rachel Mueller for their guidance and encouragement. Thanks Dr. Bangerth for your feedback on my FE model progress, and for helping me grasp difficult physical concepts. And thanks Dr. Mueller for your kind words and support along the way!

Fourth, I would like to thank my colleagues in the CSU Biology department, especially those in the GRHAF group. It has been a pleasure to be part of such a welcoming, inclusive, and professional group, and I appreciate your efforts to uplift one another and maintain a healthy work atmosphere.

Fifth, I'm extremely grateful to the University of Washington Friday Harbor Labs for the opportunity to attend their Spring 2020 3D Slicer/Slicermorph Workshop, and thanks to Mike Itgen for being the first to encourage me to attend this workshop. I had the time of my life meeting researchers from all over the world and gaining valuable skills in digital morphology methods. This was a truly influential experience for my research interests and career.

Sixth, I would like to express my thanks to the SimScale team for answering my many questions and for providing free software that supported my entire MS thesis. This may not have been possible without your accessible, user-friendly platform.

Seventh, I would like to give special thanks to Taylor Price and Christina Calcaterra for being so emotionally supportive to me ever since we met in my first year at CSU, and for maintaining our friendship as we all pursued our dreams, even after you moved to different states. Thanks for uplifting me in the tough times and for staying in touch!

Eighth, this thesis would not have been possible without the support of Brett Minichiello, who has been an incredibly supportive partner for two years (including the entire COVID quarantine), and who helped me stay sane and comfortable throughout the many challenges we endured together.

Finally, I am grateful to my family back in California. Mom, Dad, Emily, and Megan, thanks for your unconditional love and support as I navigated through the unfamiliar waters of graduate school. Thanks to each of you for staying safe and for having the strength to pursue what makes you happy.

Funding: I would also like to acknowledge NSF-IOS-1350346 and DEB-opusgrant-1911619.

TABLE OF CONTENTS

LIST OF TABLES

CHAPTER 1 – CREATING A FINITE ELEMENT MODEL

I. Introduction

The anuran auditory system is an important evolutionary feature that allows for detection of airborne sounds. This ability helps anurans with important life functions, such as evading predators, finding mates, and assessing mate competition. Tympanic middle ears are thought to have evolved independently among vertebrates multiple times (Bolt and Lombard 2008). Therefore, it is suspected that convergent traits among the ears of vertebrates reflect fundamental principles of sound transmission to the inner ear, as well as their constraints. The ancestors of modern-day amphibians were the first vertebrates to evolve a middle ear for land-based hearing. Today's amphibians retain a relatively simple and effective middle ear structure similar to those of their ancestors, and the fundamental mechanisms of these ears may reflect those that served as foundations of hearing in terrestrial vertebrates. Among amphibians, anurans are the only extant group that possess a tympanic middle ear. Therefore, anuran ears serve as excellent model systems to study the fundamental principles of hearing and can offer insights to the evolution of more sophisticated hearing we observe in land-dwelling vertebrates today.

Anuran Sound Conduction Pathways

Anurans, and other amphibians, hear through a variety of pathways, such as through water, ground vibrations, or airborne sound. The reception of airborne sound is made possible by the tympanic middle ear, which involves the use of a tympanum (eardrum). Hearing pathways that do not involve the middle ear are referred to as "extra-tympanic" pathways. Several anuran extratympanic pathways have been proposed: 1) lung hearing, in which a sensitive patch of skin

near the lung area vibrates in response to sound, which is transmitted to the inner ear (Narins et al. 1988; Heatherington and Lindquist 1999), 2) limb hearing, in which substrate vibrations are transmitted from the forelimbs to the operculum to vibrate the oval window (Hetherington 1985) and 3) mouth hearing, in which the mouth acts as a resonance chamber to help transmit sound to the inner ear through bone conduction (Boistel et al. 2013). On land, anurans likely use a combination of tympanic and extra-tympanic pathways to sense sound vibrations. However, the focus of this study is on the tympanic pathway for hearing airborne sound.

Morphology of the Anuran Middle Ear

The tympanic middle ear of anurans can be divided into two parts, the middle ear and inner ear (Figure 1.1). Unlike mammals, anurans lack an outer ear or ear canal, and the tympanum is visibly located on the side of the head. The tympanum consists of a round or oval patch of thin skin that vibrates in response to incoming sound waves. The rim of the tympanum is attached to the tympanic annulus, a funnel-shaped structure made of cartilage. When sound reaches the tympanum, it vibrates and transmits the acoustic energy to the middle ear ossicles, the columella and extracolumella (also called the stapes and extrastapes). The first ossicle, the extracolumella (or pars externa), is a cartilaginous structure loosely attached to the center of the tympanum. In most species, a thin rod-like structure called the ascending process extends from the extracolumella dorsally and fuses with the parotic crest. The extracolumella is articulated with the columella (or pars media), a long, rod-like ossicle that extends to the inner ear. The amount of ossification in the columella varies between species (Jaslow et al. 1988). Both ear ossicles are located within a middle ear cavity, which tends to be air-filled but may also contain a mucosal fold in which the ossicles are partially suspended. The medial end of the columella is called the columellar footplate (or pars interna), which is connected to the upper half of the oval

window located on the ventral rim of the inner ear. The ventral edge of the footplate is articulated with the otic capsule (Bolt and Lombard 1985; Jaslow et al. 1988; Hetherington 1992). A cartilaginous structure called the operculum is also attached to the inner ear at the lower half of the oval window, but its function is not yet known. It may help protect the ear against loud sounds (Wever 1985) or detect ground vibrations via an extra-tympanic pathway involving the forelimbs (Hetherington 1985, Jaslow et al. 1988).

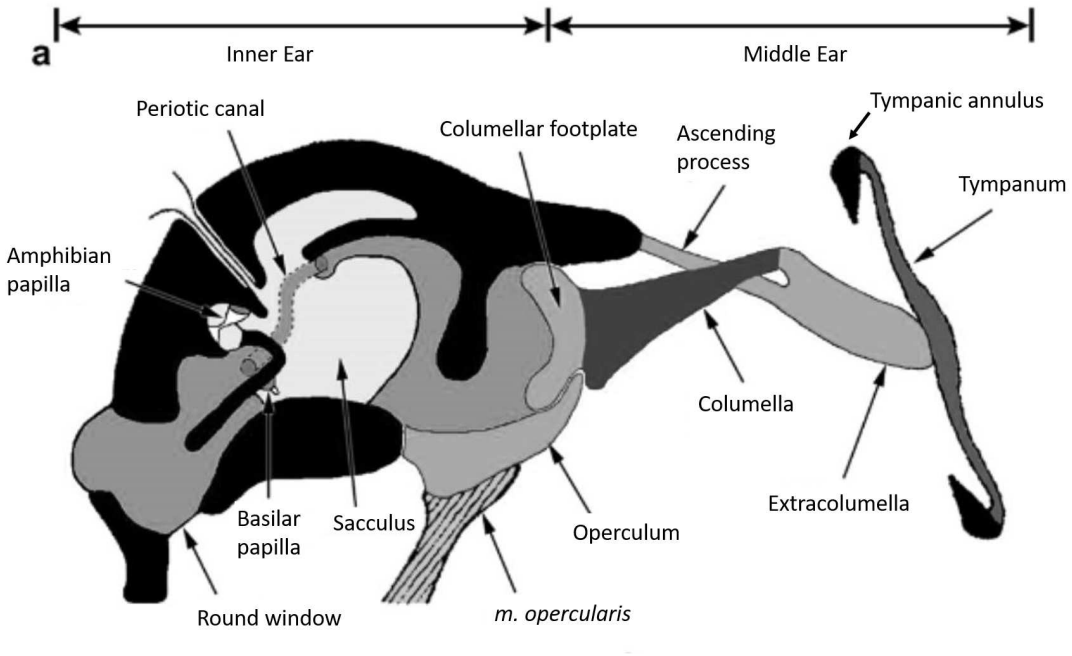

Figure 1.1: Diagram of a typical Ranid frog ear, shown in frontal section (modified from Van Dijk *et al.* 2011 and Wever 1985).

Though many advancements have been made to understand the function of the anuran middle ear, little is known about how the anuran middle ear moves in response to different sound frequencies and how differences in morphology, such as size, shape, or material properties, affect sound transmission to the inner ear. In order to approach these questions, I have created finite element (FE) models for the middle ears of two anuran species with different ear geometries. The goals of Chapter 1 are to present the first finite-element (FE) models of anuran middle ears,

which provide computational testing environments to investigate their behavior at a range of frequencies and their sensitivity to various parameters that may affect ear sound transmission. I also assess the accuracy of one of these models using empirical data, and demonstrate the utility of FE models for informing future hearing research. An awareness of the sensitivity of sound transmission to middle ear material properties could be used to understand functional variability between ears of different species and between different experimental studies.

Advantages of Computational Modeling

A computational rather than direct approach is appropriate for this study for several reasons. Middle ear structures are very small and buried within the head of an organism, which makes direct, noninvasive observation challenging. Additionally, fresh specimens are not always readily available or easy to keep in a lab environment. The ears from preserved specimens can also degrade or shrink with time, which may affect their sound transfer properties. Furthermore, the effects of some types of alterations (such as changing size or material properties) would be difficult or impossible to study in real middle ears without disrupting the ear structure. A computational finite element model surpasses these challenges by providing a reproducible test environment in which many different computational experiments can be quickly and easily tested.

Finite Element Analysis

Finite element analysis (FEA) is a rapidly growing area of biomechanics research. This type of analysis was developed by engineers in aerospace and civil engineering to simulate the performance of various designs, and began gaining popularity in the 1950s. FEA is widely used to test and predict the behavior of structures in response to different loading conditions, such as a

pressure or force. These simulations require the input of geometry, material properties, boundary conditions, and applied loads to simulation software to calculate the response of different geometries to complex loading scenarios. FEA also provides highly-accurate information about vibration shapes and stress distributions, making it a powerful visualization tool for understanding the behavior of a system. Though different theoretical modeling methods have been used to model ear mechanics, such as analytical models (Rabbitt and Holmes 1986), multibody models (Eiber et al. 2000), and analog circuit models (Hudde and Weistenhöfer 1997), finite element modeling is well-suited to simulate the complex geometry and loading regimes required for many biological applications, making it the preferred choice for computational modeling of middle ear structures.

The Finite Element Method

At the core of FEA is the Finite Element Method (FEM), a numerical technique that solves systems of partial differential equations to estimate the behavior of a structure under user-specified conditions. FEM works by using a “divide and conquer” approach, which discretizes a geometric mesh into a finite number (thousands to billions) of small parts called “elements”. The solver carries out an approximation over each element to determine their individual behavior. It then assembles these equations into a larger system of equations and solves this system to approximate the behavior for the entire system. Postprocessing steps are then used to analyze the quantities of interest, such as deformations or strains. The results are often visualized on the geometry using color scales, animations, or vectors, which show the distribution of stresses or the movement of the system in response to the applied load. An overview of this process is shown in Figure 1.2

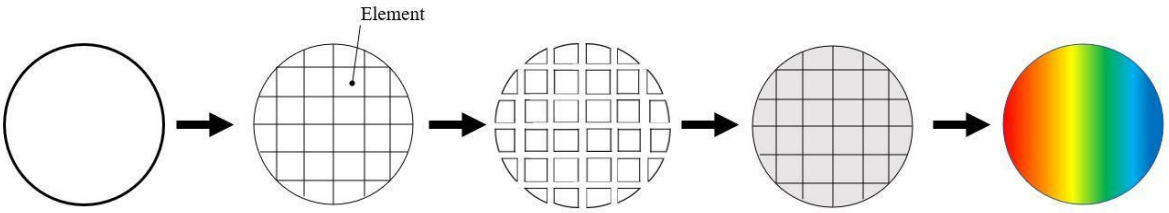

Figure 1.2: A 2D representation of the FEM Process. a) System of interest for FE modeling b) system divided into elements c) Approximation over each element d) Reassembly of elements to model the entire system e) Analysis of deformation or strains.

Harmonic Response Analysis for Middle Ear Simulations

Harmonic response analysis is a type of FE analysis used to study the response of a solid system to sinusoidal loads of a fixed frequency. This can be used to measure the response of a geometry to excitation over a range of frequencies, which makes it a useful tool for ear research. Harmonic response analysis has been used to study the frequency response of several different mammalian middle ears, including those of humans (Beer et al. 1999; Prendergast et al. 1999; Koike et al., 2002; Sun et al. 2002; Gan et al. 2004; Nie et al 2011; Wang et al. 2011; Higashimachi and Toriya, 2015; O'Connor et al. 2017; Motallebzadeh et al., 2017a; Liu et al. 2019), cats (Ladak and Funnell 1996; Tuck-Lee et al. 2008), gerbils (Elkouri et al. 2006, Maftoon et al. 2015), pigs (Hoffstetter et al. 2011) and chinchillas (Wang and Gan 2016). Many of these studies have focused on biomedical applications: Human models of the middle ear have been used to simulate sound transmission in both healthy and pathological morphologies by varying the structures and properties. This literature has taught us that finite element models can accurately represent middle ear function and are useful for biomechanical studies. This study presents the first finite element models created for amphibian middle ears, which may enable us to examine similarities and differences between independently-evolved ears and study the fundamental features and mechanisms required for tympanic hearing.

Species Descriptions

The geometry of ear components is known to vary across the order Anura. Therefore, there may also be a variety of mechanisms by which anuran middle ears work. To study these potential differences, I selected two anuran species with different ear geometries: *Rhinella marina* and *Arthroleptis tanneri*, with the intention of comparing their movement and footplate displacement over a range of frequencies. Descriptions of each species are provided below.

Rhinella marina (Figure 1.3), commonly known as the cane toad, is a species of toad native to South and Central America. It is the largest species of toad, with a snout-ventral length typically between 85-150 mm. They have distinct tympanums and complete middle ears. The advertisement call of males consists of a fast-paced stream of pulses with a dominant frequency of 517 Hz and a frequency range of 110-1180 Hz (Bleach *et al.* 2015). The specimen used for this study was likely female due to its size (roughly 10 cm) and dorsal coloration.

Arthroleptis tanneri (Figure 1.3), also known as the Tanzania screeching frog or Tanner's squeaker, is a leaf-litter species of frog endemic to montane forests of northeastern Tanzania. These frogs typically measure 35-50 mm snout-ventral length, and the tympanum is distinct (Grandison 1983). The calling frequencies of *A. tanneri* are unknown; However, Mercurio (2009) shows that southeast African *Arthroleptis* species typically have one call note at 1,600-4,900 Hz and a higher pulsed note at 4,600-7,500 Hz. The sex of the specimen used for this study was unreported.

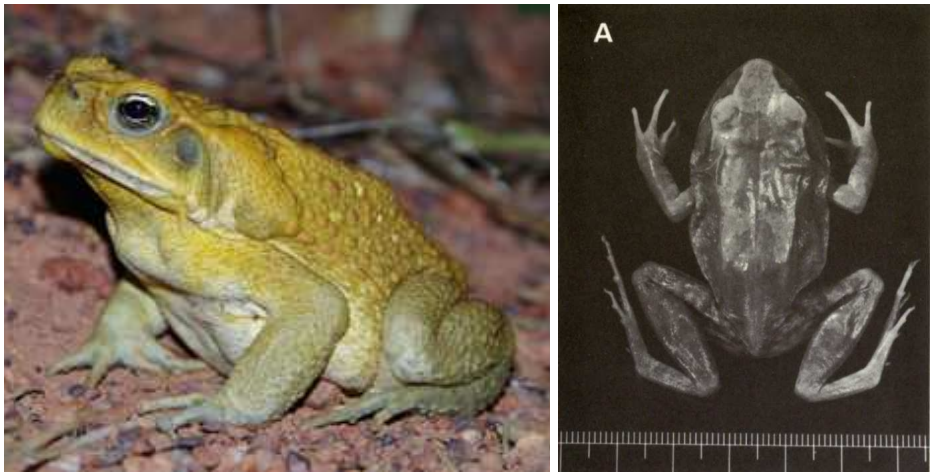

Figure 1.3: Left: *Rhinella marina* (Brown *et al.* 2015). Right: Male *Arthroleptis tanneri* (Grandison 1983).

II. Methods

There are four main steps to Finite Element modeling: Obtaining the geometry, preprocessing, solving, and postprocessing (Figure 1.4).

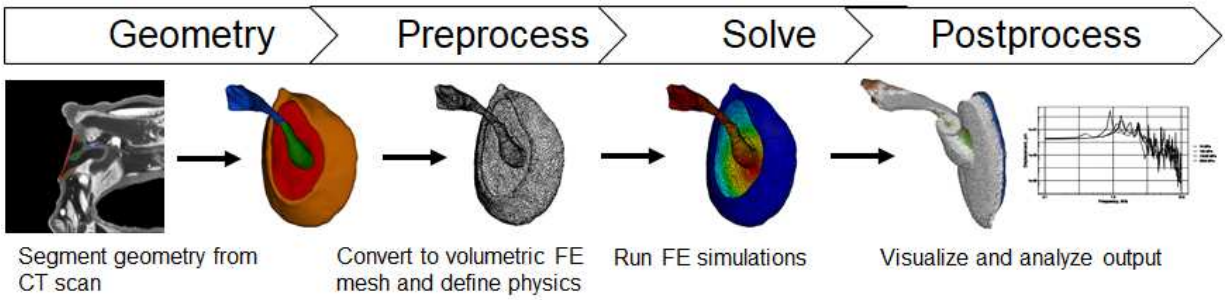

Figure 1.4: Overview of the FE modeling workflow.

Segmenting Geometry from CT Scans

Middle ear components were segmented from high-resolution CT scans to obtain accurate geometries. Diffusion iodine contrast enhanced (diceCT) scans of *Rhinella marina* (omnh:amphibians:46722.0, ark:/87602/m4/M43259) and *Arthroleptis tanneri* (cas:herp:168823,

ark:/87602/m4/M25583) were accessed through the online CT repository Morphosource.org. The left ears of both scans were reconstructed into a 3D surface mesh in 3D Slicer (Fedorov et al. 2012) using the Slicermorph extension (Rolfe et al. 2020) and segmentation tools. The slice view for each ear within the CT scans is shown in Figure 1.5, and the resulting 3D segment volumes are shown in Figure 1.6. Step-by-step instructions for this workflow can be found in Buser et al. (2020).

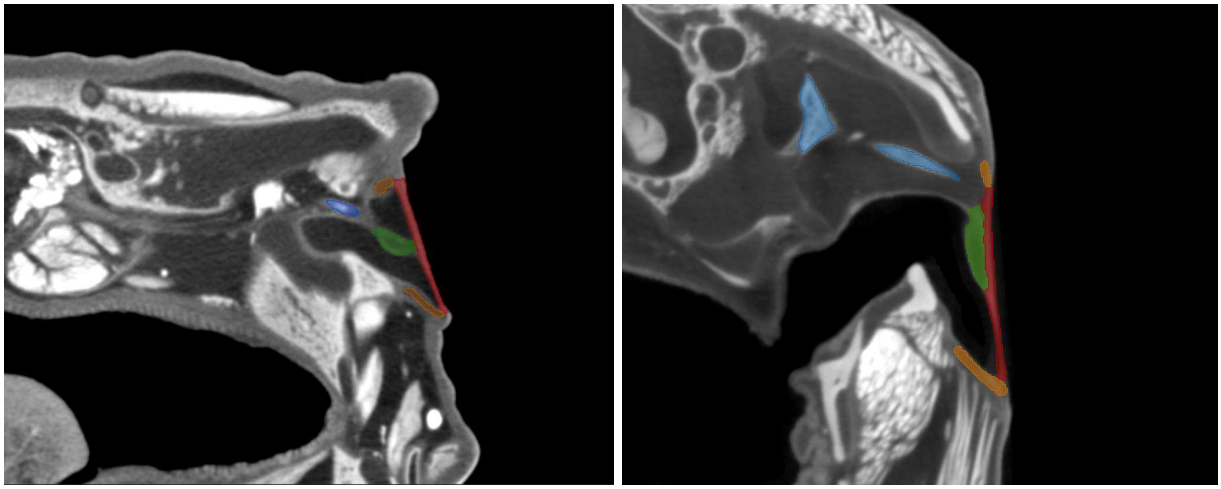

Figure 1.5: Slice view of ear segments within their CT scans, labeled with colors: Tympanum (red), tympanic annulus (orange), extracolumella (green), columella (blue). Left: Transverse plane of *R. marina*. Right: Transverse plane of *A. tanneri*.

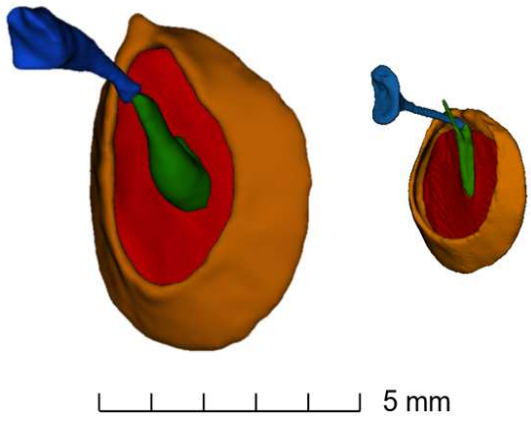

Figure 1.6: 3D models reconstructed from the CT scans. Left: *Rhinella marina*. Right: *Arthroleptis tanneri*.

Mesh Cleaning and Preparation

Following segmentation, the surface meshes were repaired, refined and smoothed in Meshmixer and Meshlab (Cignoni et al. 2008). Since surface meshes (shells) only convey information about boundaries, the surface meshes were converted into volumetric meshes. This was achieved by converting each part into a solid in FREECAD and saving them as .iges files. These files were then imported to OnShape as an assembly. The orientation of the parts in these assemblies were preserved from those of the original specimens such that no re-assembly was required. The assemblies were saved in parasolid file format (.x_t) and imported to SimScale for tetrahedral meshing and finite element analysis. Figure 1.7 shows the tetrahedral meshes generated for each species.

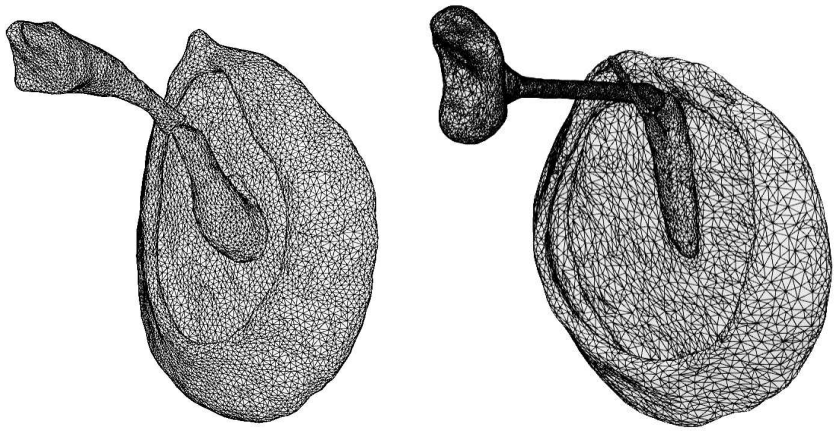

Figure 1.7: 3D finite element models with wireframe mesh showing the tetrahedral elements. Left: *Rhinella marina*. Right: *Arthroleptis tanneri*. The *A. tanneri* model is shown as being the same size as *R. marina* for easier visualization of the mesh.

Modeling Individual Ear Components

Since all models require simplification, decisions about the geometry and other properties were made for each ear component. The geometry, parameters, and simplifications for each part are described below. Measurement data for individual components can be found in Table 1.1.

Tympanum: The tympanum of the *R. marina* model measures approximately 5.7 mm tall by 4.5 mm wide, consistent with the description in Wever (1985). The segmented tympanum had an average thickness of 0.25 mm, with thickness ranging from about 0.15-3.5 mm. In *A. tanneri*, the tympanum was approximately 2.5 mm in diameter and 0.07-0.15 mm thick. Since changes in the structure of the tympanum are known to affect sound transmission, decisions about modeling the tympanum are particularly important to consider. Aernouts and Dirckx (2012) showed that in gerbil tympanums the responses to small strains behaved linearly. In this study, the strain magnitudes are small and the tympanum is assumed to have linear behavior. The tympanum material properties are also assumed to be homogeneous and isotropic due to limitations of the FE software. However, this assumption likely does not have large effects since O'Connor et al. (2017) found that, if the human tympanum is modeled as having isotropic material properties, a Young's modulus value of around 20 MPa results in sound transmission comparable to experimental values.

Tympanic annulus: The tympanic annulus (TA) was given cartilaginous properties. In both species, a bonded contact was added between the TA and tympanum, and a large fixed support was added to the outward-facing rim where it attaches to features surrounding the middle ear cavity (also see "Simulation Setup - Boundary Conditions").

Extracolumella: The exact shape of the extracolumella for *R. marina* was estimated since cartilage had poor contrast in the CT scan and was difficult to distinguish from the surrounding loose connective tissue. The extracolumella of *R. marina* may typically have an ascending process, but one was not observed while segmenting the specimen in this study.

Columella: The columella was clearly visible in both CT scans and was modeled as a solid, homogeneous bone. The level of ossification is known to vary throughout a single columella, with the highest level of ossification in the center. The upper half of the columellar footplate is made of cartilage but was also modeled as bone for simplicity.

Other simplifying assumptions: Cochlear fluid was omitted from the model since this was not expected to have a noticeable influence on the model behavior (as discussed in O'Connor et al. 2017), and it is unlikely that including this feature would change the conclusions of the study. The mucosa surrounding the ear ossicles was also omitted for simplicity. The middle ear cavity was omitted from the model for two reasons: 1) Software limitations, since the pressure was directly applied to the tympanum rather than from a point source, such that including a middle ear cavity would not simulate the effects of resonance 2) The empirical study to which the results are compared was performed with the open mouth of frogs to prevent resonance.

Summary of Species Differences in Middle Ear Geometry

The ear geometry between *R. marina* and *A. tanneri* differs in size and shape (Figure 1.8). The ear of *A. tanneri* is approximately half the size of the ear of *R. marina*. In addition to their difference in size, the columella of *A. tanneri* is relatively thin and rod-like compared to the thicker, curved columella of *R. marina*. Perhaps the biggest difference in shape can be attributed to the extracolumella of *A. tanneri*, which is rather unusual in that it lies flush with the

tympanum and extends from the center to the dorsal rim of the tympanum. By contrast, the extracolumella of *R. marina* extends proximally and dorsally such that the columella attaches farther away from the tympanum. The TA of *R. marina* also has a completely closed outer ring compared to *A. tanneri*, and the tympanum is a more oblong shape.

Table 1.1: Dimensions of ear components in *R. marina* geometry

Structure	***R. marina* Model**	***A. tanneri* Model**
Tympanum		
Diameter (mm)	~4.5	~2.5
Surface area (mm^2)	43.9	10.6
Thickness (mm)	~0.25	~0.07-0.15
Volume (mm^3)	4.5	0.46
Tympanic annulus		
Surface area (mm^2)	41.3	14.5
Volume (mm^3)	4.7	0.88
Extracolumella		
Surface area (mm^2)	6.9	1.5
Volume (mm^3)	1.1	0.08
Columella		
Length (mm)	~4.5	2.25
Footplate width (mm)	~ 1.1	0.6
Length of footplate (mm)	~1.4	0.09
Surface area (mm^2)	9.3	2.7
Volume (mm^3)	1.5	0.18

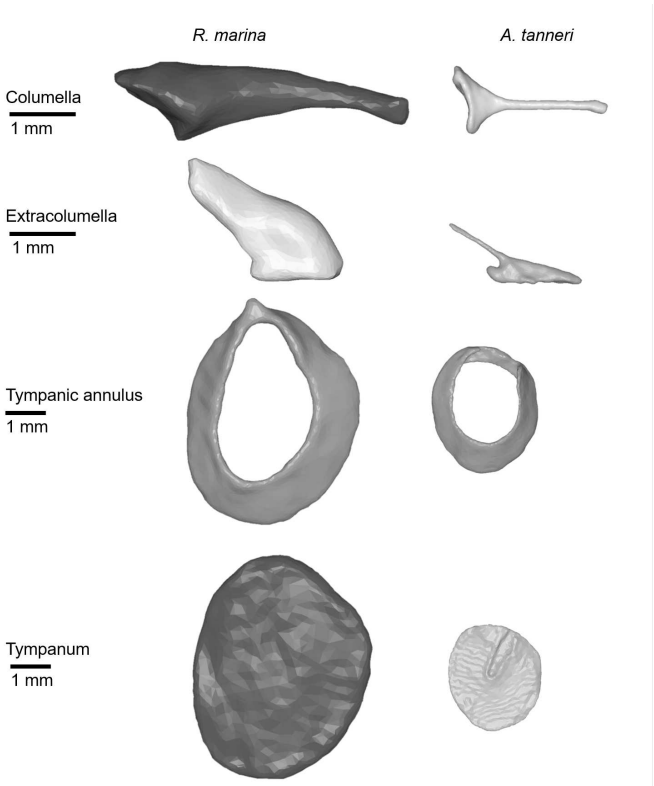

Figure 1.8: Comparison of the size and shape of geometric models from each species.

Simulation Setup

Finite Element Mesh Generation: The assembly was imported into SimScale for tetrahedral meshing and finite element analysis. Since the fineness of the mesh affects FEA results, the finest mesh setting in SimScale was used. In general, the finer the mesh, the more accurate the results but the higher the computational cost. First-order elements were used since second-order elements are far more costly in terms of time and computation, and it was determined that the use of second-order elements had little impact on the results. The final FE model consisted of 97.1k cells and 26.6k nodes. Inspection of the tetrahedral mesh showed that the elements had low aspect ratios and had overall good quality.

Material Properties: Since material properties for anuran ear components have not yet been reported, the material properties were assigned based on previously published data for human ear components (see Table 1.2). The sensitivity of the model output to the Young's modulus and density of each part is analyzed in the results section to test the effect of these assumptions.

Table 1.2: Mechanical properties used in the baseline FE simulation for each species.

Structure	Parameter	Model
Tympanum	Density (kg/m^3)	1200[a]
	Young's modulus (MPa)	20[b]
	Poisson Ratio	0.3[a]
	Rayleigh damping	
	α (s^{-1})	0[a]
	β (s)	1.0×10^{-4} [a]
Tympanic annulus	Density (kg/m^3)	1200[a]
	Young's modulus (MPa)	0.6[a]
	Poisson Ratio	0.3[a]
	Rayleigh damping	
	α (s^{-1})	0[a]
	β (s)	7.5×10^{-5} [a]
Extracolumella	Density (kg/m^3)	1080[c]
	Young's modulus (MPa)	7.2[c]
	Poisson Ratio	0.3[a]
	Rayleigh damping	
	α (s^{-1})	0[a]
	β (s)	7.5×10^{-5} [a]
Columella	Density (kg/m^3)	4350[a]
	Young's modulus (MPa)	13440[a]
	Poisson Ratio	0.3[a]
	Rayleigh damping	
	α (s^{-1})	0[a]
	β (s)	7.5×10^{-5} [a]

[a]Liu et al. 2019, [b]O'Connor et al. 2017, [c]Brummund et al. 2014

Boundary Conditions: A pressure load of 100 dB SPL (2 Pa) was applied to the lateral side of the tympanum (Figure 1.9). Fixed supports were assigned based on the morphology and connections of the middle ear components with the surrounding middle ear cavity: A fixed support was applied to the TA around the outside of the ring (Figure 1.9), and an elastic support was added along the ventral edge of the columellar footplate to model its articulation with the otic capsule. Since the rigidity of this connection is unknown, the FE model was then cross-calibrated with the *R. marina* footplate displacement data from Saunders and Johnson 1972. The spring constant for this support was set to 500 N/m, the value at which the footplate displacement (at low frequencies) was low enough to approximately match that of the empirical data. Empirical data for displacement has not yet been reported for *A. tanneri*, so no validation study was performed.

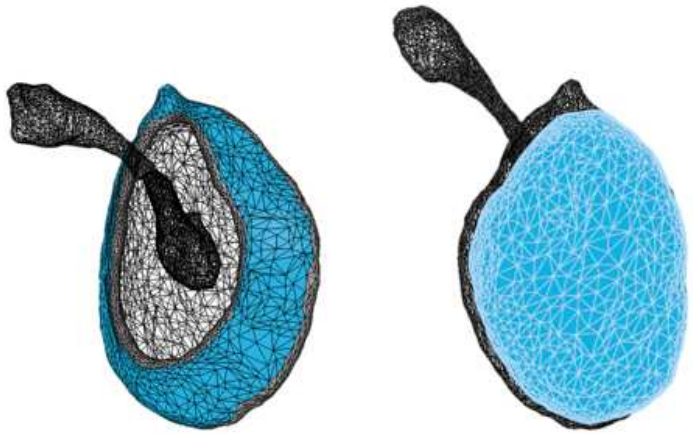

Figure 1.9: *R. marina* fixed support and applied pressure, highlighted in blue. Left: Fixed support around tympanic annulus. Right: Applied pressure load on the lateral side of the tympanum (blue).

Contacts: Two bonded contacts were assigned: one between the tympanum and tympanic annulus, and one between the extracolumella and columella. A sliding contact was used between the tympanum and extracolumella to represent the loose connection between these components.

Finite Element Analysis

Harmonic response analysis was performed from 100 to 10,000 Hz with an interval of 100 Hz. The magnitude of displacement was measured for points on the center of the tympanum and the center of the columellar footplate. The Poisson's ratios of the middle ear elements were assumed to be 0.3 for all materials since published Poisson's ratios for ear components are close to this value (Elkhouri et al. 2006; Koike et al. 2002; Sun et al., 2002). The Rayleigh damping parameters alpha and beta for all materials of the middle ear were assumed to be alpha = 0 s^{-1} and beta = 0.000075 s based on Liu et al. 2019. The displacement data were analyzed by plotting the magnitude (absolute value) of the displacements against the frequency.

III. Results

R. marina

Distribution of Displacement

As shown in Figure 1.10, the magnitude of displacement has an unequal distribution throughout the middle ear. At low-mid frequencies (up to about 4 kHz), the areas of highest displacement are just below the center of the tympanum and throughout the ossicular chain, with some variation in the amount of displacement throughout the ossicles. The displacement decreases outward from the center of the tympanum until it reaches the TA. The TA shows zero displacement due to the fixed support surrounding the outer portion of the ring. A similar pattern is observed for most other frequencies below 4 kHz. At higher frequencies, the displacement in the ossicular chain is lower and the displacement pattern on the tympanum becomes highly variable. For more details on the patterns of movement, see Chapter 2 Results.

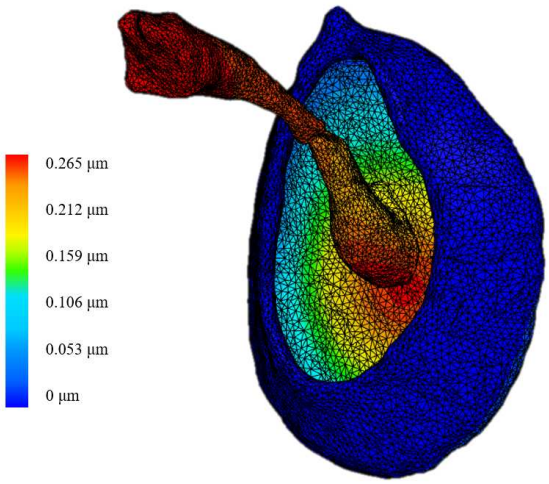

Figure 1.10: Magnitude and distribution of displacement in the *R. marina* model in response to a sound frequency of 1 kHz.

Frequency Response Curve with Baseline Settings

The magnitude of displacement at a range of frequencies, or the frequency response function, was measured for *R. marina* (Figure 1.11). The vocalization range for *R. marina* has been shown to vary between about 110-1180 Hz (Bleach et al. 2015), and footplate displacement is highest within this range. It is also interesting to note that the hearing and vocalization range for frogs typically does not exceed 4-5 kHz, by which point the displacement has dropped significantly. The sharp peaks seen in the model are the result of resonance from the various structures in the model.

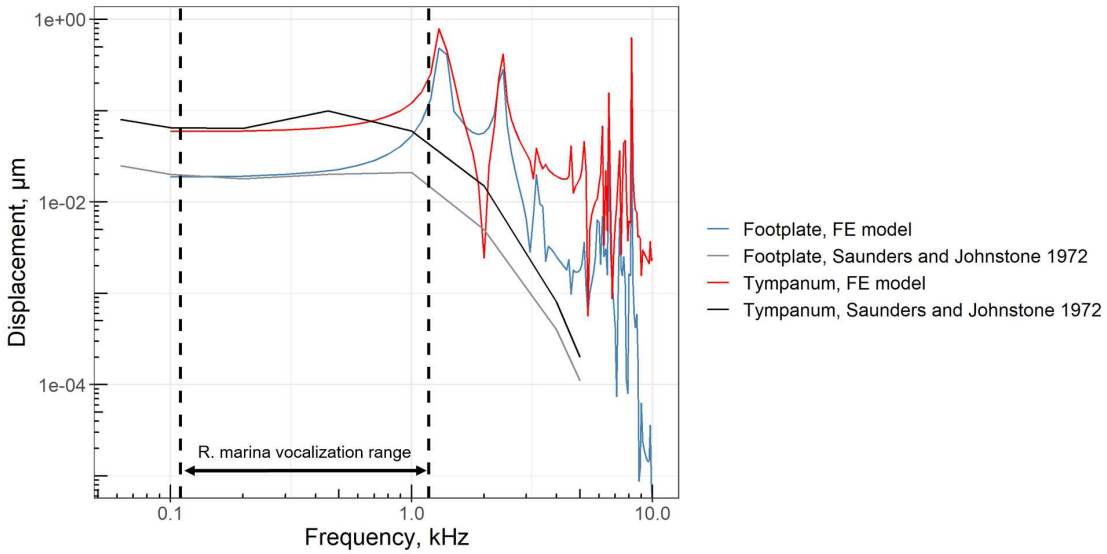

Figure 1.11: Baseline frequency response curve for *R. marina*. The frequency range for male vocalizations is shown between the dotted vertical lines. The greyscale lines represent data estimated from Saunders and Johnstone 1972 in which the frequency response of *R. marina* tympanum and columellar footplate were directly measured.

Model Validation

The model for *R. marina* was validated by comparison to published data from Saunders and Johnstone 1972. In this study, the Mossbauer technique was used to measure the amplitude of displacement of the tympanum and columellar footplate for *Rhinella marina* and *Hyla dentata* for the frequency range 67-4,000 Hz at 100 dB SPL. Figure 1.11 shows the comparison between the data measured in this study and the finite element model frequency response function. The magnitude of the response of both the footplate and tympanum closely resembles the empirical data within the *R. marina* vocalization range, and both curves begin to drop off at approximately 1 kHz. However, the responses from the model appear to drop off at a slower rate. The FE data also show sharp resonance peaks, which may indicate lack of damping compared to a real ear response. It is also possible that these peaks were averaged out in the empirical study due to individual variation.

Discrepancies between the empirical data and the simulated data could be due to several factors. The first is the modeling of the TA, since O'Connor et al. 2017 found that an inflexible TA typically results in increased transmission at high frequencies. It is possible that the fixed support of the TA is more rigid than in reality and could be increasing the high-frequency response. More empirical data about the connection between the TA and tympanum, and any vibration of the TA, would be of use for future models. Another potential factor could be that the middle ear ossicles in the model are not embedded in loose connective tissue. In a real ear system this may have a role in the damping of sound, which would potentially smooth the resonance peaks seen in the model.

Next, the density and Young's modulus (elasticity) of each ear component were varied independently to test the range of influence that these parameters have on the model function, and to determine whether more precise measurements are needed to optimize the model. This was performed with the *R. marina* model, and repetition with key parameters in *A. tanneri* (not shown) was generally found to produce similar patterns. For each plot, the baseline response is shown in black and colors show deviation from the baseline at higher or lower parameter values.

Effects of Varying Young's Modulus

Tympanum

The Young's modulus of the tympanum was systematically varied from 1 MPa to 100 MPa (Figure 1.12). As the Young's modulus increases, the footplate displacement significantly decreases at frequencies lower than 3 kHz. A right shift in the peaks also occurs. These simulations reveal that the choice of tympanum Young's modulus can have a relatively high impact on sound transmission to the inner ear, especially at frequencies below approximately

3kHz, which is within the normal hearing range of most frog species.

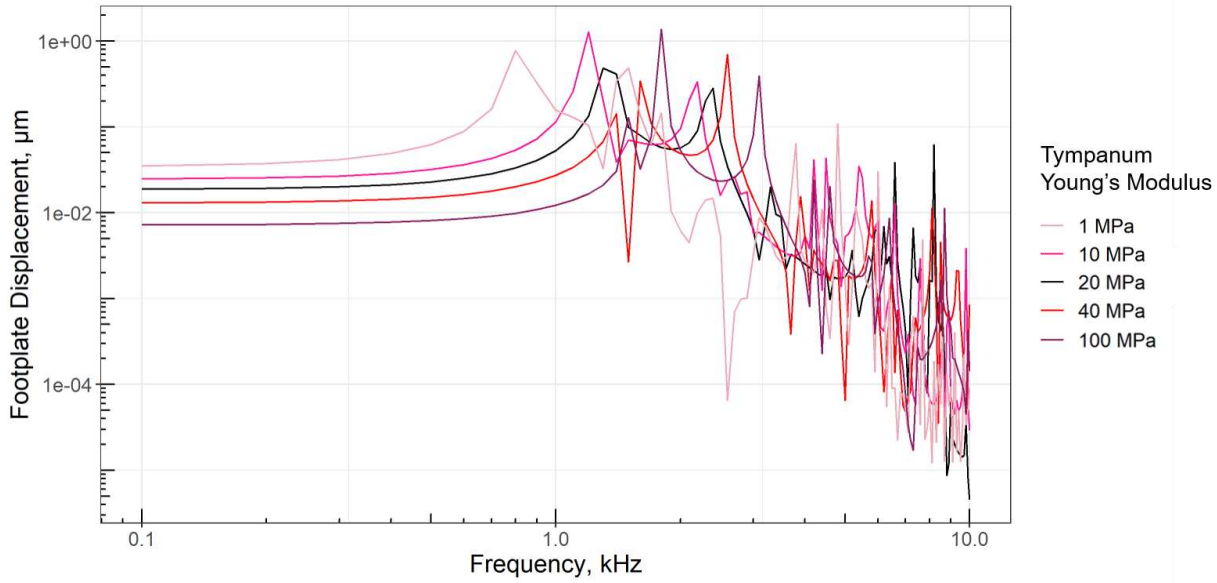

Figure 1.12: Footplate displacement frequency response curves for various Young's modulus values applied to the tympanum.

Tympanic annulus

The Young's modulus of the tympanic annulus was varied from 0.1 MPa up to 100 MPa (Figure 1.13). Increasing the Young's modulus had a substantial effect on lowering the footplate displacement at low frequencies, consistent with the results of O'Connor el al. 2017 for human ear models. This suggests that having a flexible, cartilaginous tympanic annulus may be important for optimizing sound transmission to the inner ear within the frog hearing range.

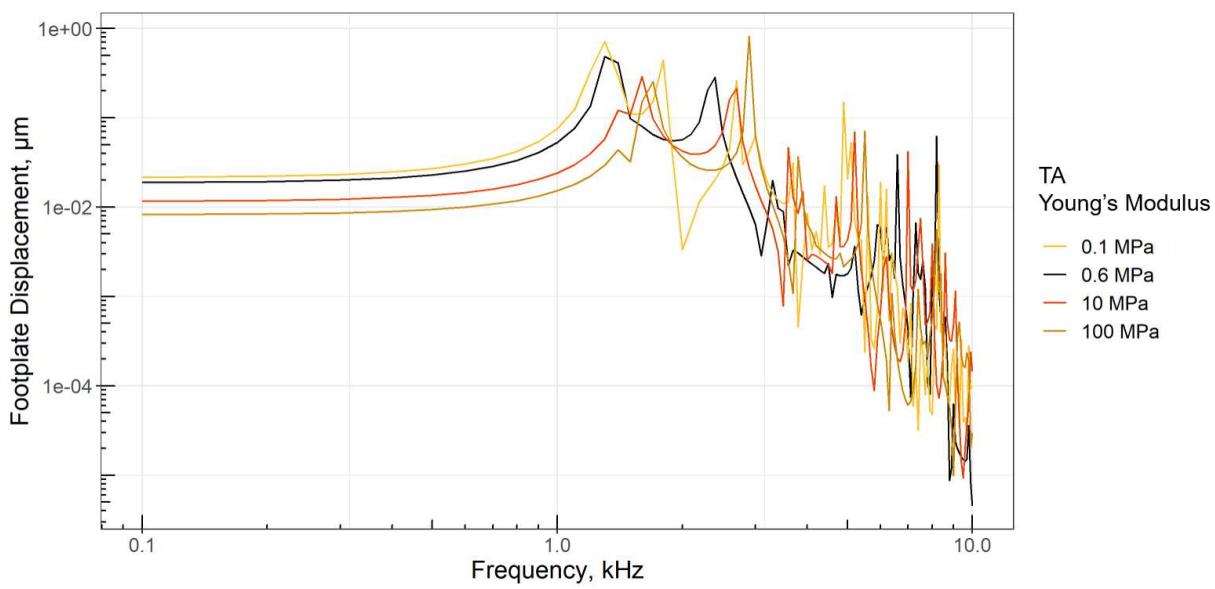

Figure 1.13: Footplate displacement frequency response curves for various Young's modulus values applied to the tympanic annulus.

Extracolumella

The Young's modulus of the extracolumella was found to have a moderate influence on the response. Lowering of the extracolumella Young's modulus significantly reduced the footplate displacement across the frequency range (Figure 1.14), however, increasing the Young's modulus even by a large amount had very little effect on the response. This suggests that the values used for this parameter could potentially have a large impact on the response if this structure is less stiff than predicted. It also suggests that having even a small amount of stiffness in this structure is critical for proper sound transmission.

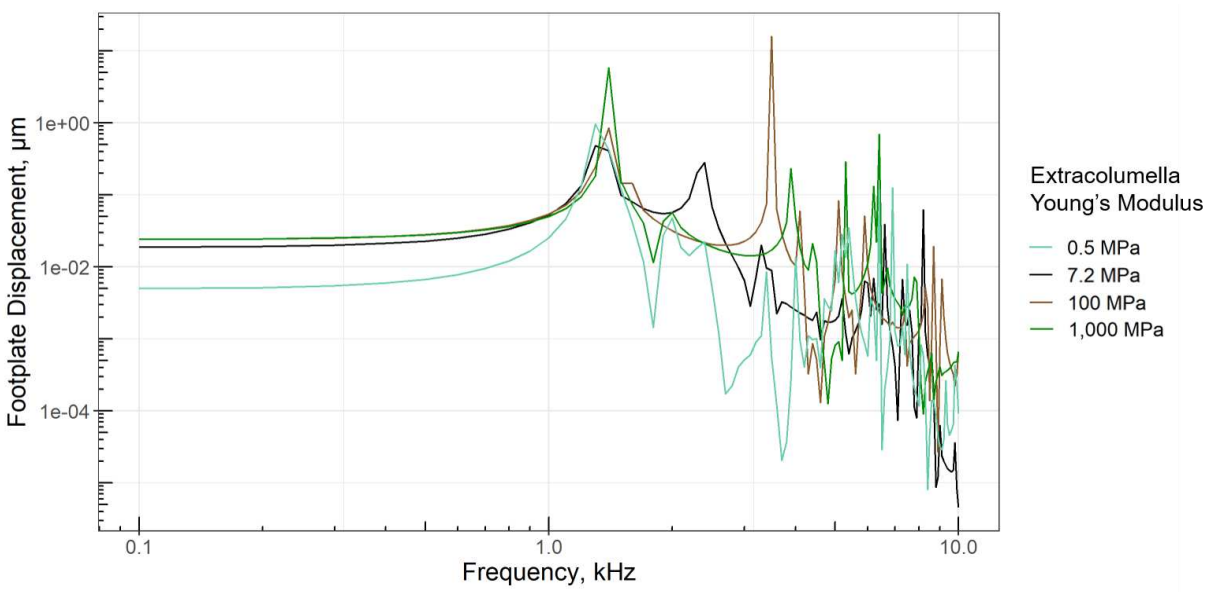

Figure 1.14: Footplate displacement frequency response curves for various Young's modulus values applied to the extracolumella.

Columella

The Young's modulus of the columella was varied between 10-20,000 MPa (Figure 1.15). The footplate displacement was mostly affected by changes in Young's modulus when the value became small (10 MPa), approaching the values used for cartilage in this study. Even at this low value, the magnitude of displacement was not greatly affected. Increasing the Young's modulus to 20,000 MPa also had little effect on the response. This suggests that the level of ossification in the columella may not be one of the most important factors in sound transmission.

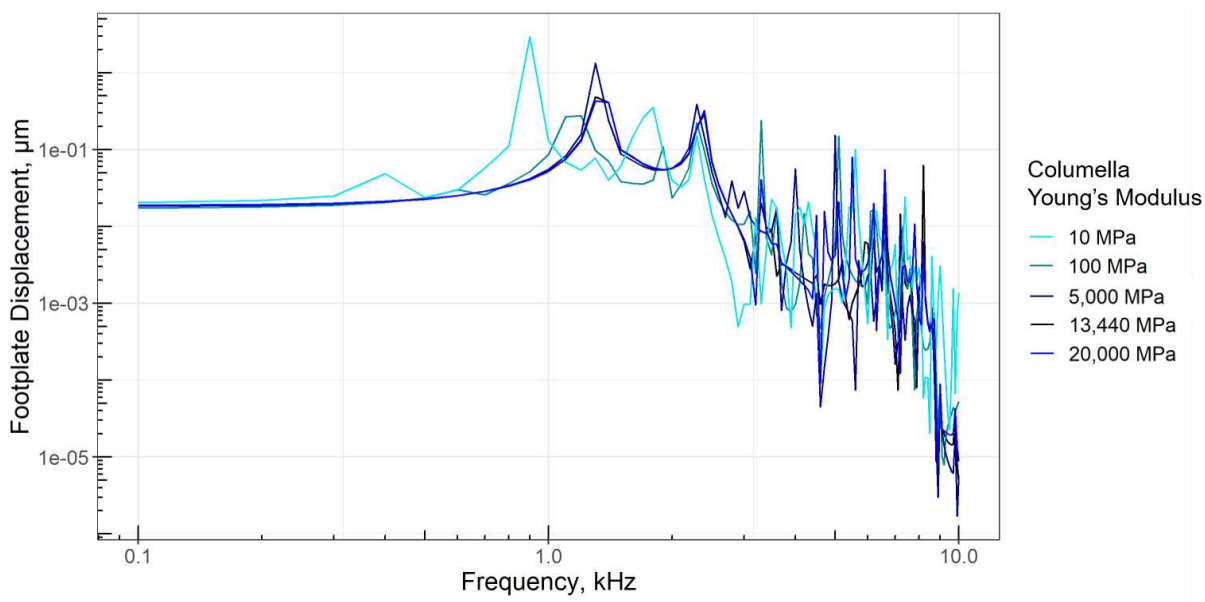

Figure 1.15: Footplate displacement frequency response curves for various Young's modulus values applied to the columella.

Effects of Varying Density

The effects of varying mass can be achieved by varying density. In general, varying density resulted in very little difference in footplate displacement at low frequencies, and more variation at higher frequencies (see O'Connor et al. 2017). Since the frog middle ear essentially works as a mass-spring system, it is expected to be more sensitive to changes in mass at higher frequencies (Funnell et al. 2013).

Tympanum

Altering the density of the tympanum appears to have a moderate influence on the footplate response (Figure 1.16). There is a small shift toward lower frequencies as density increases, which is expected since an increase in mass decreases the resonance frequency of a structure.

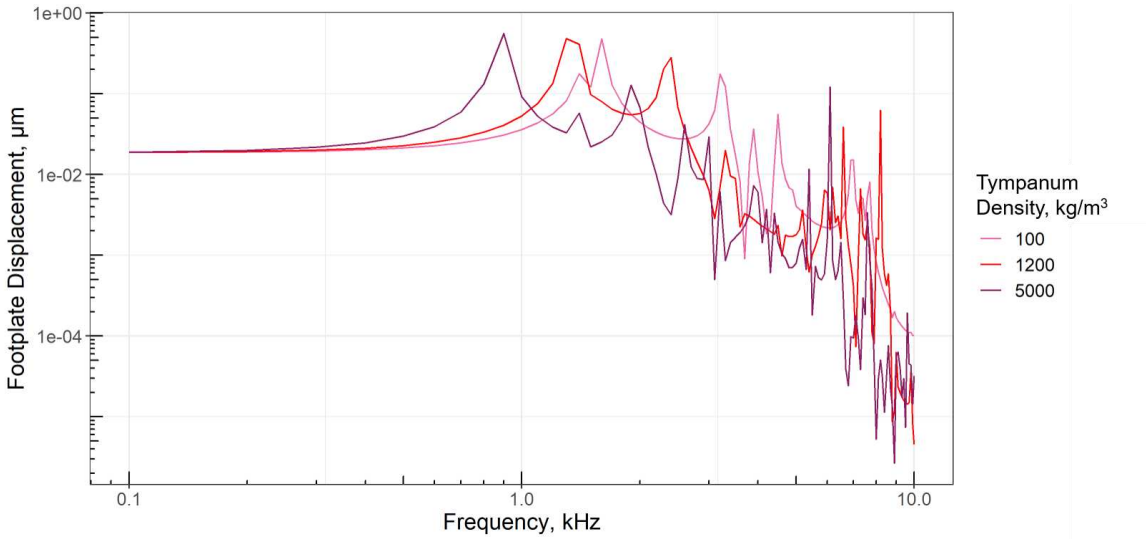

Figure 1.16: Footplate displacement frequency response curves for various density values applied to the tympanum.

Tympanic annulus

Varying the density of the TA had no effect on the response at frequencies below 3 kHz, and little effect on frequencies higher than this value (Figure 1.17). The relatively low effect of altering density compared to the other parameters may be due to the relatively minor role the tympanic annulus has in sound transfer apart from supporting the tympanum.

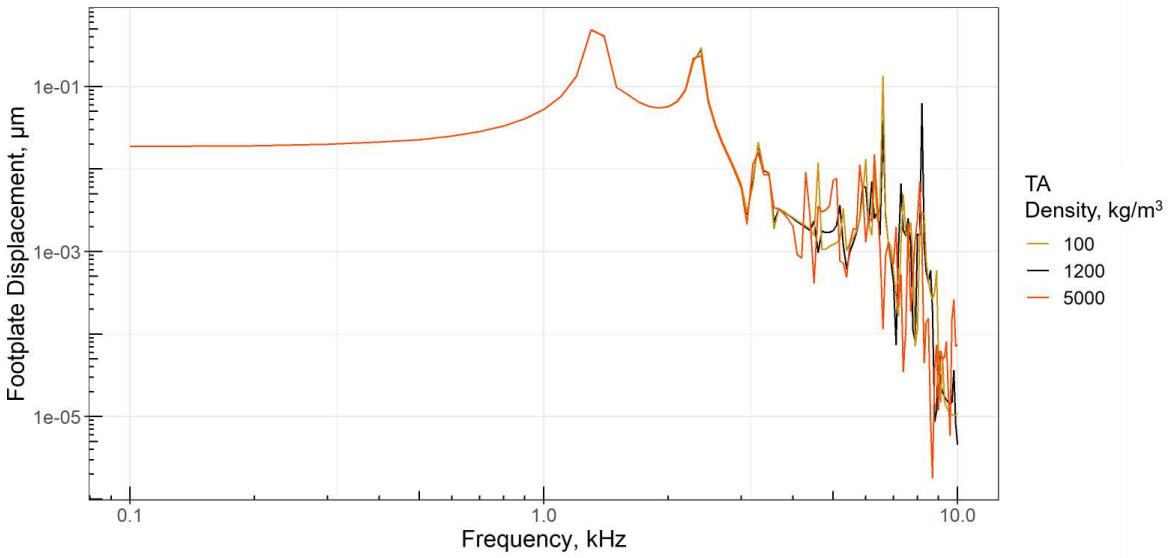

Figure 1.17: Footplate displacement frequency response curves for various density values applied to the tympanic annulus.

Extracolumella

As with the tympanum, increasing density of the extracolumella caused a small shift of resonance peaks toward lower frequencies (Figure 1.18). The magnitude of displacement was relatively unaffected at low frequencies, and more variation was observed at higher frequencies.

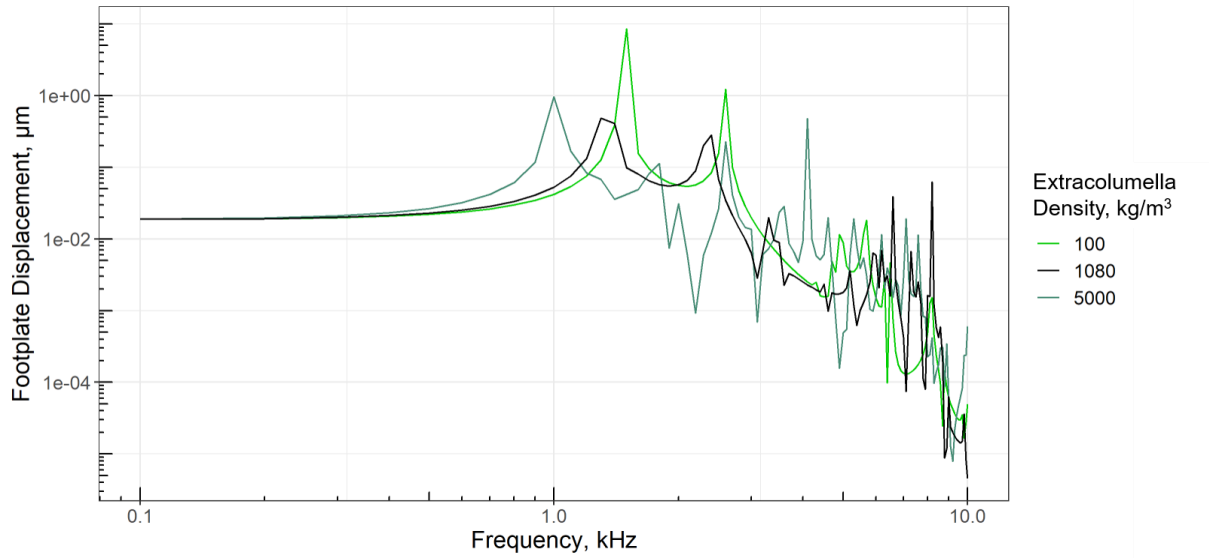

Figure 1.18: Footplate displacement frequency response curves for various density values applied to the extracolumella.

Columella

Decreasing the density of the columella to 100 kg/m3 had a considerable effect on the displacement at high frequencies (Figure 1.19) but little effect on frequencies less than 3 kHz. Increasing the density shifted the resonance peaks toward lower frequencies.

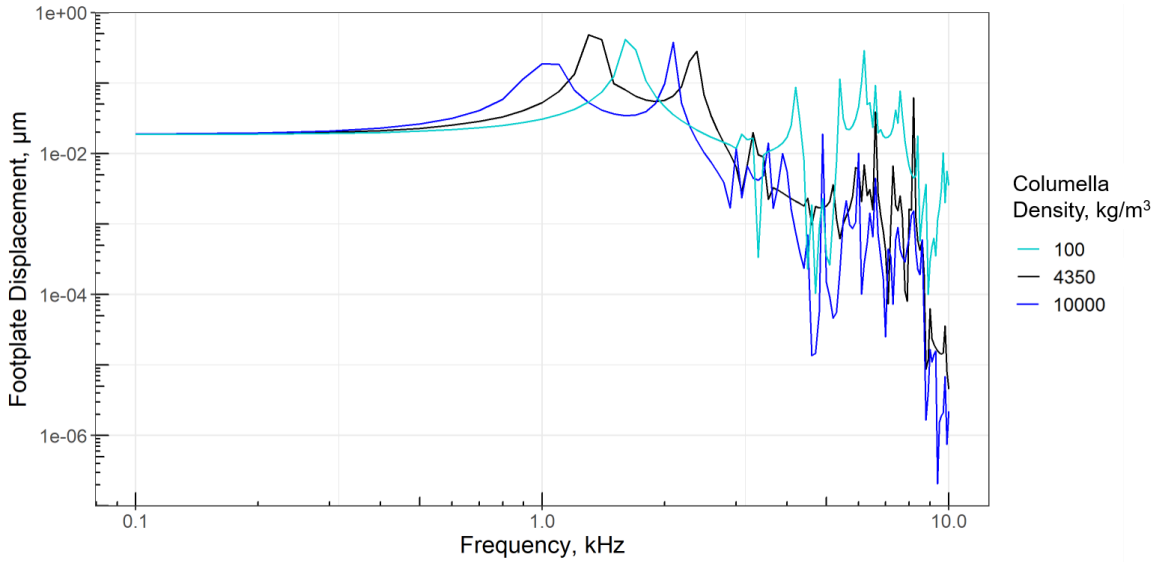

Figure 1.19: Footplate displacement frequency response curves for various density values applied to the columella.

Effects of a Cartilaginous vs Bony Extracolumella

Unlike mammalian ears, in which all the ear ossicles are composed of bone, the ears of birds, reptiles, and amphibians have one cartilaginous ossicle: the extracolumella. To test the potential advantages of having this cartilaginous ossicle, the extracolumella was assigned the same Young's modulus and density as the bony columella. The FE model predicts that having a cartilaginous extracolumella slightly decreases the footplate displacement in the hearing range of *R. marina* compared to the bony extracolumella (Figure 1.20). It is possible that having a cartilaginous columella plays a role in extending the high displacement range to almost 3 kHz. Though the difference in displacement was overall subtle, Chapter 2 shows that there are consequences for the mode of movement as a result of changing this parameter.

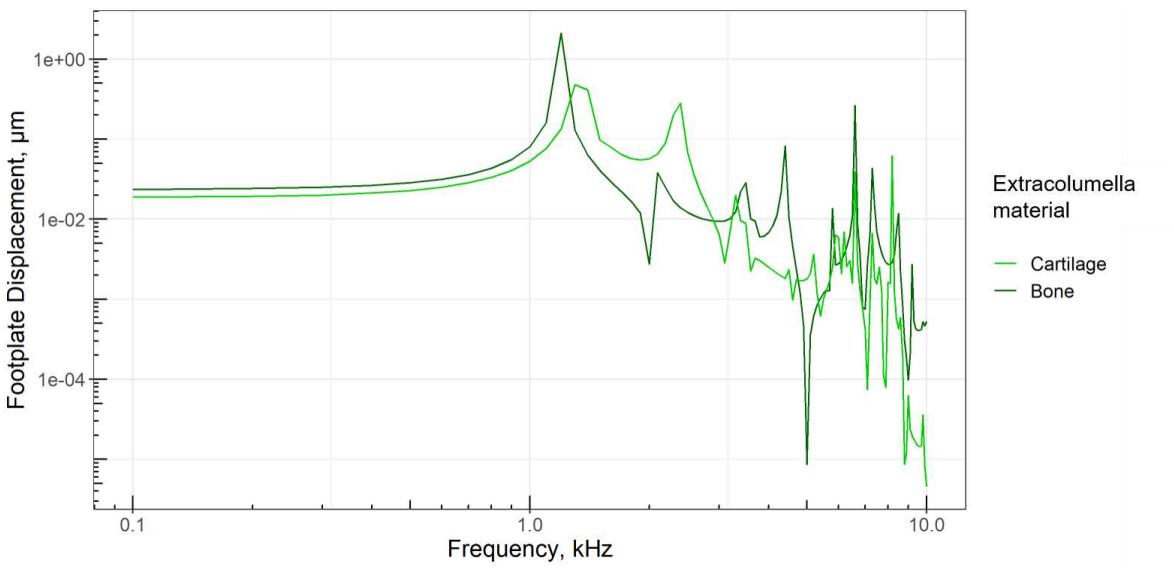

Figure 1.20: Frequency response curves showing the difference in footplate displacement between a cartilaginous and bony extracolumella.

Elastic Footplate Support

To capture the effects of the articulation between the columellar footplate and the otic capsule, a small elastic support was used on the ventral edge of the footplate. An elastic rather than fixed support was selected to allow for rotation about this axis and to allow for adjustment of the strength of this connection. This adjustment is done through alteration of the spring constant k, which was varied to test the effect on rigidity of movement and footplate displacement. It was found that this had a substantial impact on the footplate displacement at frequencies below approximately 3 kHz (Figure 1.21). Visual inspection of the model animation showed that this connection becomes essentially rigid once k reaches approximately 2,000 N/m. As previously mentioned, the baseline model was cross-calibrated with empirical data from Saunders and Johnstone 1972 to select this parameter (500 N/m) since this connection has not

yet been studied in detail. These data suggest that the nature of this connection is extremely important for the overall function of the middle ear.

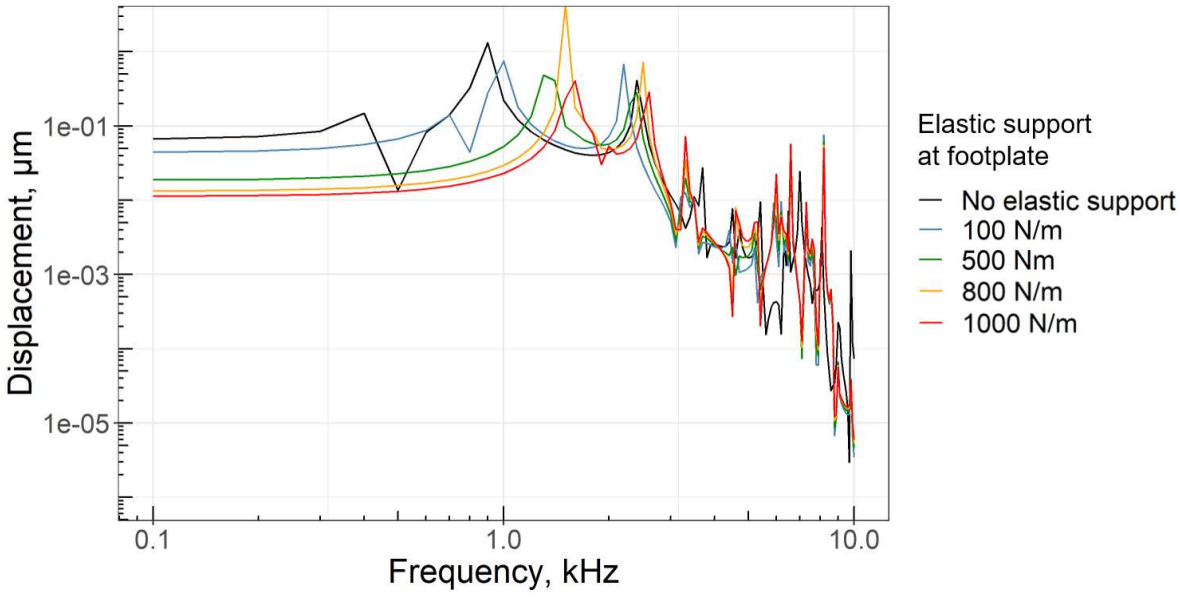

Figure 1.21: Effect of varying the spring constant (k) of the elastic footplate support on footplate displacement.

Poisson Ratio

The Poisson Ratio is defined as the expansion of a material in the direction perpendicular to compression. This ratio for most materials is between -1 to 0.5, with 0.2-0.5 considered incompressible. The effect of the Poisson Ratio used for middle ear FE models generally varies from 0.3 to 0.35. The effect of using higher and lower Poisson Ratio values on sound transmission was tested by altering the ratio for all ear components simultaneously. It was found that this change in Poisson Ratio has very little effect on the response other than the magnitude of the resonance peaks (Figure 1.22). This suggests that the exact value of Poisson Ratio has little overall influence on the behavior of the model.

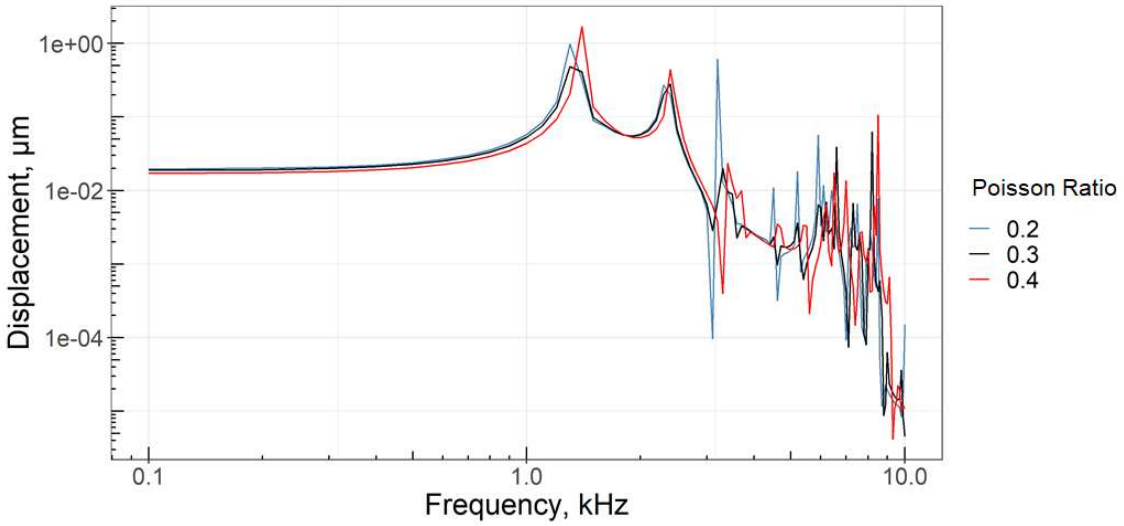

Figure 1.22: Frequency response curves showing the difference in footplate displacement when the Poisson ratio for all ear components are changed simultaneously to 0.2 or 0.4.

A summary of the results in this chapter is shown in Table 1.3.

Table 1.3: Summary of Chapter 1 results.

Structure	Parameter	Influence	Trend
Tympanum	Young's modulus	High	Strong inverse relationship with displacement magnitude at frequencies below 3 kHz.
	Density	Moderate	Increase in density causes shift toward low frequencies.
Tympanic annulus	Young's modulus	High	Increase in Young's modulus results in decrease in displacement magnitude and resonance peak shift toward higher frequencies. Opposite effect for decrease in Young's modulus.
	Density	Very low	No effect on displacement below 3 kHz. Little effect at frequencies greater than 3 kHz.
Extracolumella	Young's modulus	Moderate	Decrease in Young's modulus lowers displacement magnitude. Increase causes the second resonance peak to shift toward higher frequencies but very little increase in displacement magnitude.
	Density	Low	Increase in density causes a slight shift toward lower frequencies. The opposite trend occurs for decrease in density.
Columella	Young's modulus	Low	Changes in Young's modulus have little effect until it becomes less than 100 MPa, then it shifts toward lower frequencies. Little effect on the magnitude of displacement.
	Density	Low	Increase in density causes a slight shift toward lower frequencies and less steep dropoff at high frequencies.
	Footplate Elastic Support	High	Increase in k causes significant decrease in displacement below 3 Hz.
All Structures	Poisson Ratio	Very low	Changes to 0.2 or 0.4 results have little effect on displacement across the frequency range.

Arthroleptis tanneri Results

Distribution of Displacement

The distribution of displacement in the *A. tanneri* model (Figure 1.23) is similar to that observed in *R. marina*. The largest amount of displacement is typically just below the center of the tympanum, with a decrease as it radiates outward toward the rim. There is a moderate amount of displacement in the ear ossicles, with some variation at the extracolumella. There is no displacement at the fixed support around the TA or at the fixed tip of the ascending process.

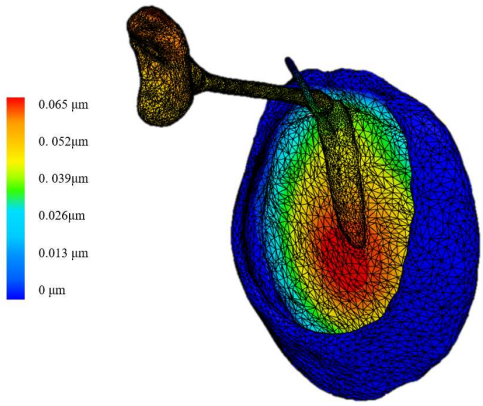

Figure 1.23: Distribution of displacement in the *A. tanneri* model at 1 kHz frequency.

Baseline Frequency Response Function

The frequency response function for *A. tanneri* has steady displacement between 100-1,000 Hz, increases to a maximum displacement range between 1,000-4,000 Hz and then begins to decline at higher frequencies (Figure 1.24). As previously mentioned, Mercurio 2009 shows that southeast African *Arthroleptis* species typically have one call note at 1,600-4,900 Hz and a higher pulsed note at 4,600-7,500 Hz. The FE results show that the lower frequency call note is mostly aligned with the highest displacements, but the higher pulsed note is not.

It is important to note that empirical data for displacement was not available for this species, and it is possible that the model does not accurately represent the entire hearing range of *Arthroleptis*. It is also possible that the high-displacement range is accurate, but that *A. tanneri* has a lower frequency pulsed note than other *Arthroleptis* species that is within range of the highest displacements (up to approximately 4 kHz). The spring constant for the elastic support on the ventral edge of the footplate was specified as the same as for *R. marina* (500 N/m), though this value may be different for this ear. Because of the uncertainty about this parameter, and because it greatly alters the amount of displacement of the footplate at low frequencies, the difference between the tympanum and footplate displacement will not be compared to that of the baseline *R. marina* model. Variation due to the Young's modulus and density were not analyzed in detail for this species since initial results on key parameters showed similar patterns to that of *R. marina*.

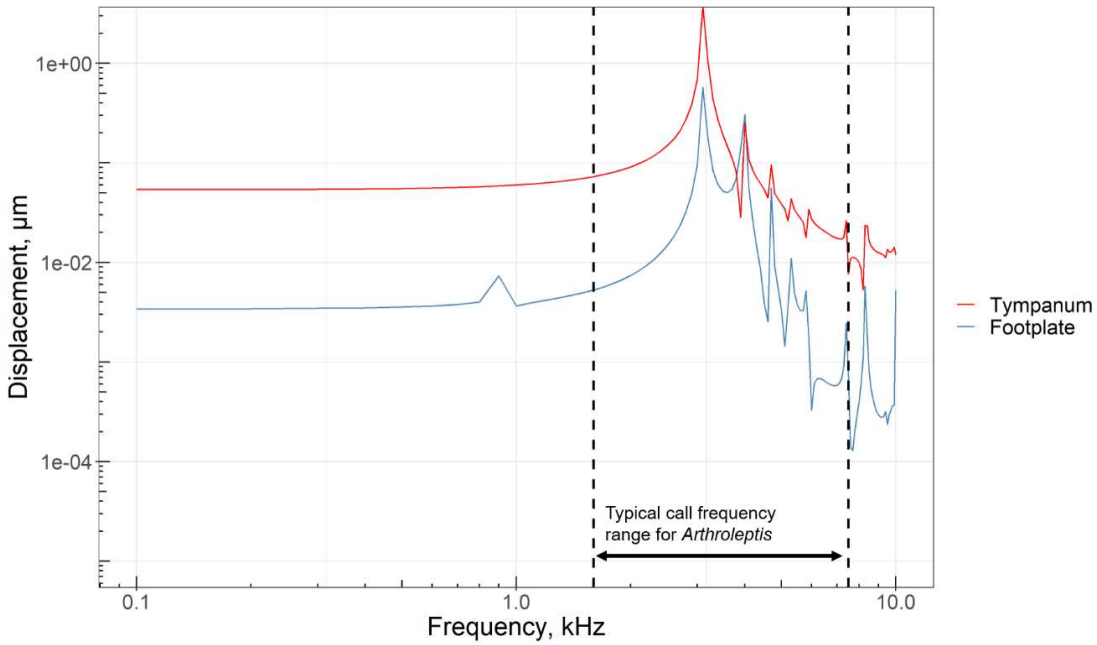

Figure 1.24: Frequency response curves showing the footplate and tympanum displacement for the baseline *A. tanneri* FE model. The predicted vocalization range for *A. tanneri* is shown between the dashed lines.

Species Comparison

Next, I compared the footplate displacement of *R. marina* and *A. tanneri* (Figure 1.25). Although the overall displacement in *A. tanneri* is lower, the frequency range in which displacement is relatively high extends to much higher frequencies than *R. marina*: the high-displacement range for *A. tanneri* reaches up to approximately 5 kHz before dropping off, compared to about 1 kHz in *R. marina*. The direction of this difference in sensitivity corresponds with that of the calling range for each species suggesting that perhaps the middle ear is tuned to frequencies within range of the vocalizations (or vice versa). Since the material properties were the same between models, this difference in frequency sensitivity could be due to either the size or geometry of the ear components. The next section controls for the effect of size on the frequency response.

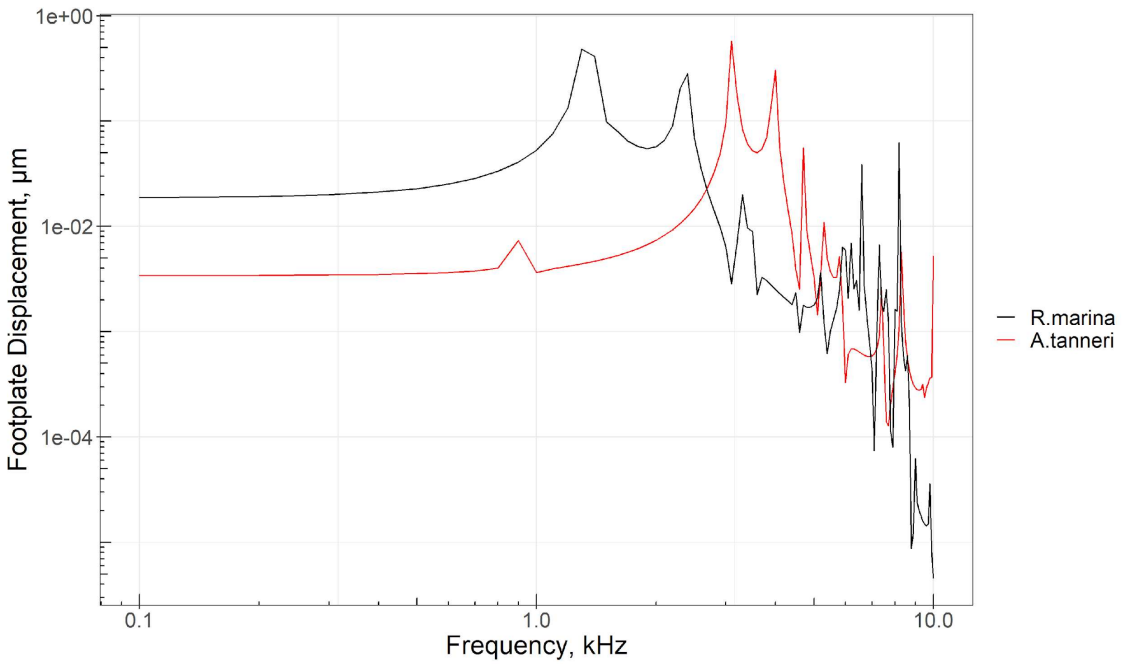

Figure 1.25: Frequency response curves showing the difference in footplate displacement between the baseline *R. marina* and *A. tanneri* FE models.

Comparison Between Species at a Similar Size

To test the effects of size on the frequency response function, I measured the diameters of the *R. marina a*nd *A. tanneri* tympanums to determine the ratio of their sizes, which were approximately 5 mm and 2.5 mm, respectively. I then applied a scaling factor of 0.5 to *R. marina* to scale the model to the approximate size of the *A. tanneri* ear. The simulation results show that, at similar sizes and with the same material properties, both ears have similar frequency response curves (Figure 1.26). The *R. marina* ear response is slightly higher compared to *A. tanneri*, but the overall pattern is fairly similar. Since the scaling factor was approximate, it is possible that the curves could be even more similar with a different or more precise measure of size. Nonetheless, these results suggest that size, rather than morphology, is likely the main factor contributing to the shape of the frequency response curve.

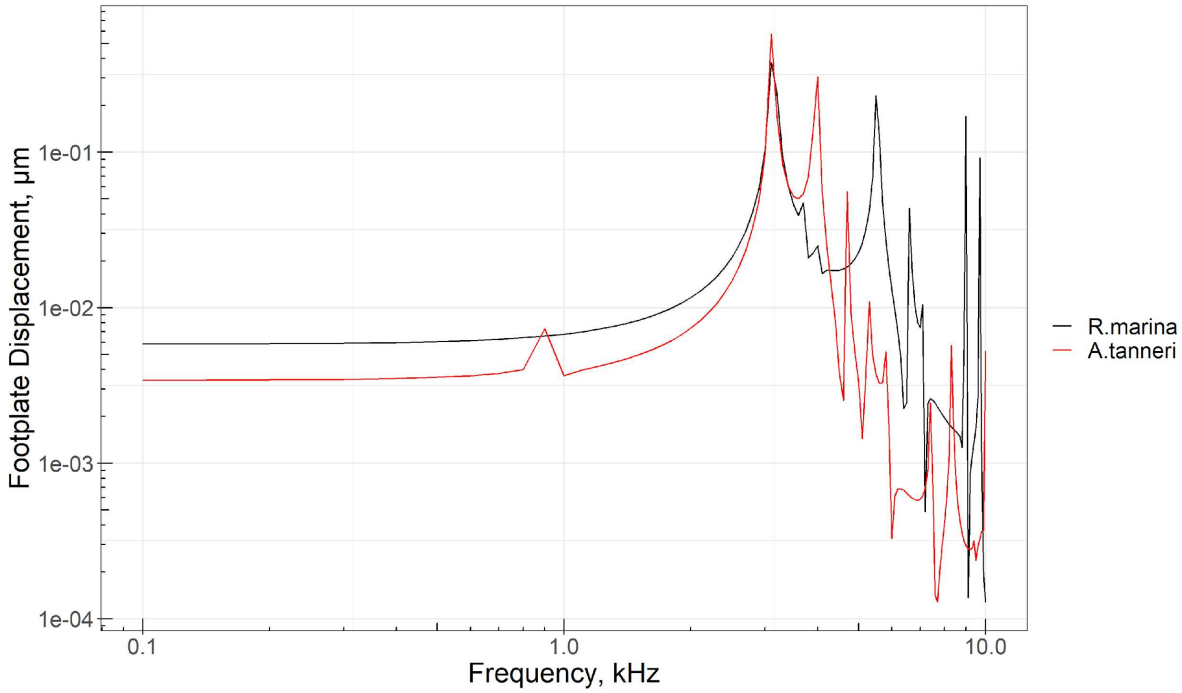

Figure 1.26: Frequency response curves showing the difference in footplate displacement between the *R. marina* FE model scaled by 0.5 and *A. tanneri*.

IV. Discussion

Understanding the extent to which various factors impact middle ear FE models can help us understand functional variability in the ears of amphibians or other vertebrates and lead to new hypotheses about the adaptive benefits of the material properties found in one or more ear parts. Though the models provide some new insights, there may be differences in movement that displacement data does not capture. Chapter 2 addresses how middle ear movement changes throughout the frequency range in the baseline model and as a result of varying different model parameters.

It is important to note that the amount of displacement at a range of frequencies does not entirely represent the ability of an organism to hear within this frequency range. The middle ear works as a broadband filter of sound from the environment, and sound that passes to the inner ear is further filtered and processed. The sensory epithelia in the inner ear are tuned to different frequencies and largely determine the frog's sensitivity to any given frequency. Due to the large amount of interspecific variation in inner ear morphology, it is difficult to predict how sound transmitted from the middle ear is processed for any individual species (Smotherman and Narins 2004). Further research on frog inner ears would be helpful in understanding the fate of vibrations transmitted from the middle ear.

The results suggest that the stiffness level of the columella does not affect the output in a significant change in footplate displacement, even when the Young's modulus is very low. A lack of sensitivity to columella stiffness may have important implications for understanding development, as this suggests hearing ability may not be strongly affected if the columella is still ossifying post-metamorphosis. However, empirical data (Womack et al. 2016) show that

developing post-metamorphic toads experience an increase in hearing ability upon ossification of the columella and thickening of the tympanic annulus. It is possible that the columella material properties matter more in a real system, or it could be that thickening of the tympanic annulus is much more influential than columellar ossification. Further tests are required to determine whether one or both of these factors are necessary for proper ear function.

Another important point to discuss is that the ear response of frogs in the empirical study by Saunders and Johnstone (1972) was measured with an open mouth cavity to reduce resonance. This allows for the FE model to match the direct measurements more closely since the simulations also do not capture the effects of resonance. However, Chung et al. 1981 showed that the mouth cavity and eustachian tubes impact the tympanum response by acting as Helmholtz resonators. In that study, laser vibrometry was used to measure the tympanum displacement of bullfrogs at a range of frequencies with and without the mouth open. The results showed that with the mouth closed, there was a large additional peak in displacement for frequencies between 1-2 kHz. Therefore, it is likely that the FE models do not account for a major range of displacement that may influence the predicted hearing response for either species. Interestingly, Chung et al. also showed that it is possible to predict the range of this extra displacement using the volume and cross-sectional area of the resonance cavity. Future work could explore the frequencies at which resonance is likely to increase tympanum displacement. Overall, future studies should consider the effects of resonance in order to accurately represent frog hearing capabilities and sound transfer effects of the middle ear.

It is also worth noting that the sound pressure level used in this study, 100 dB SPL, is quite standard for these types of studies but is relatively loud compared to most sounds in nature. For reference, 30 dB is about the sound level of a whisper, and 60 dB is talking volume, and

sound levels of 120 dB or greater can cause hearing damage. Many FE studies have used 80 or 90 dB SPL, but I selected 100 dB in order to match the empirical data collected by Saunders and Johnstone 1972 for validation. A brief analysis of the effect of lowering the sound pressure level revealed that the shape of the curve remains exactly the same, but the overall displacement decreases.

Lastly, it is worth noting other implications of this study to ear research. As a result of this project, I established a FE workflow new to middle ear research that uses only free software. For biological researchers new to FE, starting a workflow for a new study is notoriously difficult, and this is a common problem for those interested in beginning such a study. In my case, development of this workflow took approximately four months, not including time spent learning CT segmentation and digital morphology. To help address this issue, I intend to share this new workflow through publication and online databases that have been created specifically for sharing FE workflows.

V. Summary and Conclusions

The FE models in this study provide an approach to understanding the underlying sound transmission dynamics. The maximum columellar footplate displacement of *R. marina* resembles the empirical data and is consistent with the vocalization frequency range for this species. At low frequencies (<4 kHz), the response was most sensitive to changes in the Young's modulus of the extracolumella and tympanum, but not the columella. This suggests that the level of ossification of the columella may not have a large impact on sound transmission. The density of the middle ear structures had little impact on the footplate displacement, especially at low frequencies. The results also indicate that having an extracolumella made of cartilage rather than bone may extend

the high displacement range for *R. marina* to almost 3 kHz. Additionally, the model was not sensitive to changes in the Poisson Ratio. The frequency response for *A. tanneri* showed an overall lower displacement, but the dropoff point occurred at higher frequencies (about 5 kHz) compared to *R. marina* (about 1 kHz). This is consistent with the vocalization range of *A. tanneri* (1,600-7,500 Hz), which is higher than that of *R. marina* (110-1,180 Hz). Finally, when size of the ear was controlled, there was little difference in the response between the ears of both species, indicating that size has far greater influence on middle ear response than the geometry.

VI. Future Directions

In order to ensure that realistic middle ear behavior is captured by the models, further improvements can be made: 1) further exploration of middle ear microstructure and connections, and 2) measuring the material properties of the ear components, especially the extracolumella and tympanum due to their sensitivity to changes in the Young's modulus. I would also recommend measuring the properties of the TA since the one used in this model had an expansive fixed support and was essentially treated as rigid. This may not be the case in a real frog ear. Another particularly important parameter to measure would be the rigidity of the articulation between the ventral edge of the columellar footplate and the otic capsule since the FE models relied on cross-calibration to select this parameter. It is probable that this articulation is more rigid than was specified in the simulations, which could have an effect on the magnitude of displacement and mode of movement.

Additionally, direct measurement of footplate displacement in *A. tanneri* would be helpful for validation of the FE model. These data would be used as a standard for comparison to help determine additional model parameters that may be important to ear function in this species.

However, given that this species is currently classified as endangered, it may be difficult to obtain specimens. Therefore, if the geometry of the *A. tanneri* ear is of interest for further research, it may be more practical to identify another more common species with similar geometry for these measurements and create an FE model of the middle ear based on this new species.

Finally, since there is great diversity in the structure of frog middle ear structures, it is likely that there is diversity in ear function as well. Comparative studies between FE models of additional species and the FE models presented here could provide important insights to the diversity in middle ear function. In particular, it may be interesting to explore the function of middle ears of species from a variety of lifestyles, including fossorial, arboreal, aquatic, and leaf-litter species. This could also provide a deeper understanding of the most fundamental features required for middle ear function, as well as their constraints.

CHAPTER 2 - ANALYSIS OF MODEL MOVEMENT AT A RANGE OF FREQUENCIES

I. Introduction

The middle ear of anurans (frogs and toads) serves as an excellent system for studying fundamental principles of hearing. This system is composed of (laterally to medially): the tympanum (eardrum), tympanic annulus, extracolumella, and columella, which collectively transmit sound to the inner ear (see Chapter 1 for an overview of ear morphology). Several studies have attempted to measure the mode of ear movement for frogs in the family Ranidae using laser vibrometry methods (Jørgensen and Kanneworff 1998, Mason and Narins 2002, Werner 2003). However, the mechanism and characteristics of sound transmission are still not well understood. Finite element (FE) models for the anuran ear can help reveal important factors for proper ear function and lead to new hypotheses for future research in frog hearing mechanics. The goal of Chapter 2 is to analyze the movement of finite-element (FE) models of anuran ears to analyze their behavior at a range of frequencies, determine how modes of movement change as a result of altering various parameters, and to compare the ear model movements to what has been described by experimental studies. The results of this study may help further our understanding of hearing in frogs and auditory systems in general.

Mechanics of Sound Transmission

The middle ear aids in sound transmission from the environment to the inner ear. In order to hear, small hair cells within the inner ear fluid must vibrate in response to sound. However, the impedance of the inner ear fluid is much higher than that of air, which results in the reflection of sound energy at the interface. To overcome this challenge, the tympanic middle ear acts as an

impedance-matching tool to increase the amount of acoustic energy that reaches the inner ear. The tympanum of most vertebrates is connected to the oval window of the inner ear by a set of ossicles made of cartilage or bone. In mammals, each of these ossicles are made of bone, whereas non-mammalian tetrapods have one cartilaginous and one bony ossicle. In anurans, these are the extracolumella and columella, respectively. Vibration of the tympanum converts sound energy from the environment into mechanical energy in the middle ear, then into fluid vibrations in the inner ear. When this fluid is moved, electrical (neural) signals are generated and sent to the brain for interpretation as sound. In amphibians, these signals are sensed by three auditory organs: The sacculus senses very low frequencies (20–120 Hz), the amphibian papilla senses low-mid frequencies (120–1250 Hz), and the basilar papilla senses high frequencies (1250–4000 Hz) (Smotherman and Narins, 2000; Christensen-Dalsgaard and Narins, 1993).

The middle ear contributes to the impedance matching between the air and inner ear fluids through pressure amplification, which can be achieved in two ways. The first is by having a smaller oval window than tympanum, thereby concentrating the force onto a smaller area. The second is by amplifying the force, which can be accomplished by the middle ear moving as a lever-like system. Both methods are generally believed to operate in vertebrate ears (Jaslow et al. 1988; Manley 1990), including the ears of anurans (Bolt and Lombard 1985; Jaslow et al. 1988). In these studies it was suggested that, in anurans, the columellar footplate rotates around its ventral edge for force amplification, which Bolt and Lombard (1985) refer to as a “pump handle” movement. The pump-handle hypothesis has been supported by empirical studies (Jørgensen and Kanneworff 1998, Mason and Narins 2002, Werner 2003), which have shown that frogs in the family Ranidae have middle ears that function as a first-order lever. In this type of mechanical system, a load applied to one end of the lever causes a pivot about a fulcrum point

and the mass on the other side moves in the opposite direction (Figure 2.1, Left). According to the pump-handle hypothesis, the fulcrum corresponds to the ventral edge of the columellar footplate (Figure 2.1, Right).

To test the pump-handle hypothesis, Jørgensen and Kanneworff used laser vibrometry to determine whether the ear of the grass frog (*Rana temporaria*) acts as a lever system to increase force amplification. This showed that the columella rotates around the articulation between the columellar footplate and the otic capsule at low frequencies (below 3,000 Hz), referred to here as the "footplate axis", which provided empirical evidence for the pump-handle hypothesis. Additionally, an outward movement of the footplate was observed directly when pressing inward on the tympanum.

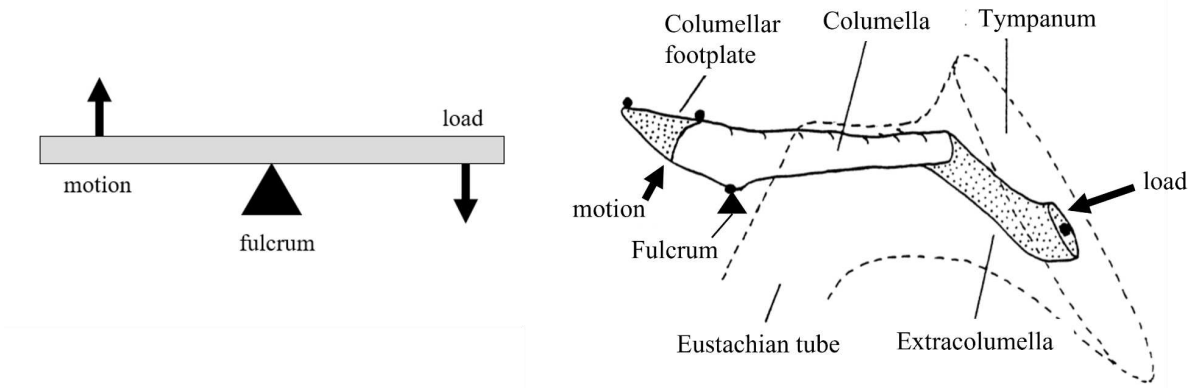

Figure 2.1: Lever systems. Left: First-order lever system. Right: Lever system in middle ear according to the pump-handle hypothesis (adapted from Jørgensen and Kanneworff 1998).

The extracolumella is also expected to play an important role in ear function. Mason and Narins (2002) used general observations and laser vibrometry to directly measure the movements of the extracolumella in association with the tympanum and columella. They observed that pressing inwards on the tympanum resulted in the extracolumella moving inwards and sliding down the tympanum due to its loose attachment. The ascending process also bends from this

motion, and there is a small amount of bending at the hinge-like connection between the extracolumella and columella. These observations were verified with vibrometric data of the extracolumella. Figure 2.2b shows the hypothesized mode of movement for an intact middle ear, in which there is rotation about both the footplate axis and extracolumella axis. The fulcrum was calculated to be located somewhere between the extracolumella and the footplate. However, the authors also postulate that the mode of movement likely varies at higher frequencies, and that the location of the fulcrum may also change with frequency, but this has not yet been confirmed. Jorgensen and Kanneworff also found that when the ascending process is severed, the ear likely rotates about a point close to the articulation of the columella and extracolumella at certain frequencies, resulting in very little displacement (Figure 2.2c). This demonstrated that the ascending process is critical for normal ear function.

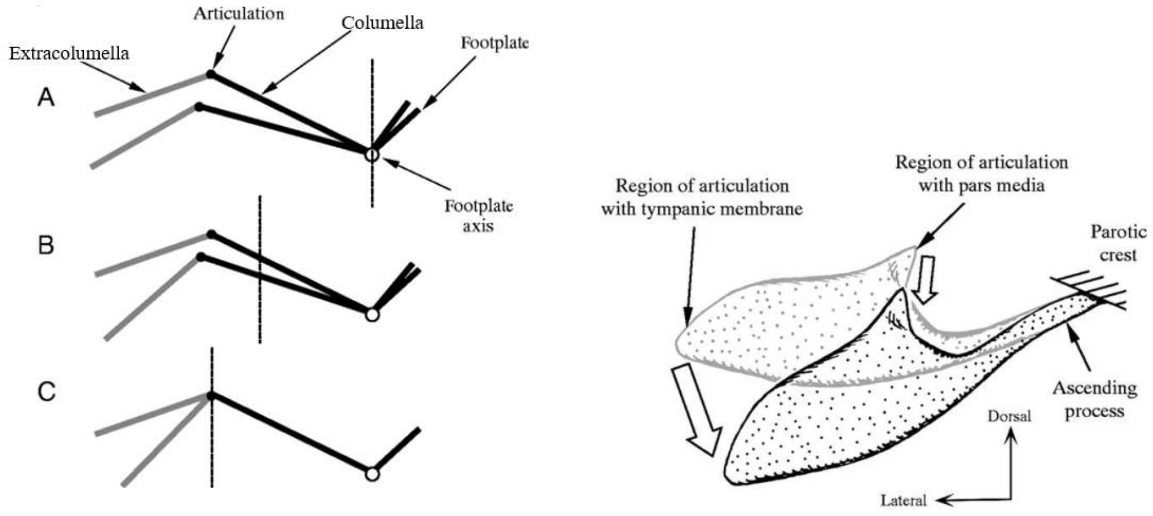

Figure 2.2: Left: Hypothetical modes of motion for the frog middle ear ossicles, exaggerated for clarity (modified from Mason and Narins 2002) a) Stiff connection between the extracolumella and columella resulting in rotation at the footplate axis b) Rotation at the footplate axis and extracolumella axis, representing the predicted movement for an intact frog ear c) Rotation about the extracolumella axis only. Right: Diagram showing the proposed movement of the extracolumella in a normal frog ear (Mason and Narins 2002).

To further explore middle ear movement and function, I analyzed the frequency-dependent vibration modes of two anuran middle ears using the finite element models developed in Chapter 1. *R. marina* was selected since its geometry closely resembles that of species used in most anuran hearing studies, and *A. tanneri* was selected due to its unusual ear geometry and the presence of an ascending process. Based on the literature, I expect to see the following features in the model animations: tympanum inflection, a downward movement of the extracolumella along the tympanum, a small hinge-like movement between the columella and extracolumella, and a rocking motion about the footplate axis. When the tympanum is inflected, I should observe the footplate to rock laterally toward the tympanum, and the opposite pattern for when the tympanum rebounds. I expect this to be the primary motion in *R. marina* for frequencies up to 3,000 Hz, and potentially extending past this range. Since the size and geometry of *A. tanneri* differs from the ears of *R. marina* and bullfrogs, I suspect that I may find differences in the modes of movement for this species or the frequencies at which they occur. Additionally, I expect to see a bending motion of the ascending process in *A. tanneri*. When the fixed support of the ascending process is removed (to mimic severing of the ascending process), I expect to see relatively little displacement of the *A. tanneri* footplate. A visual summary of these expected movements is shown in Figure 2.3.

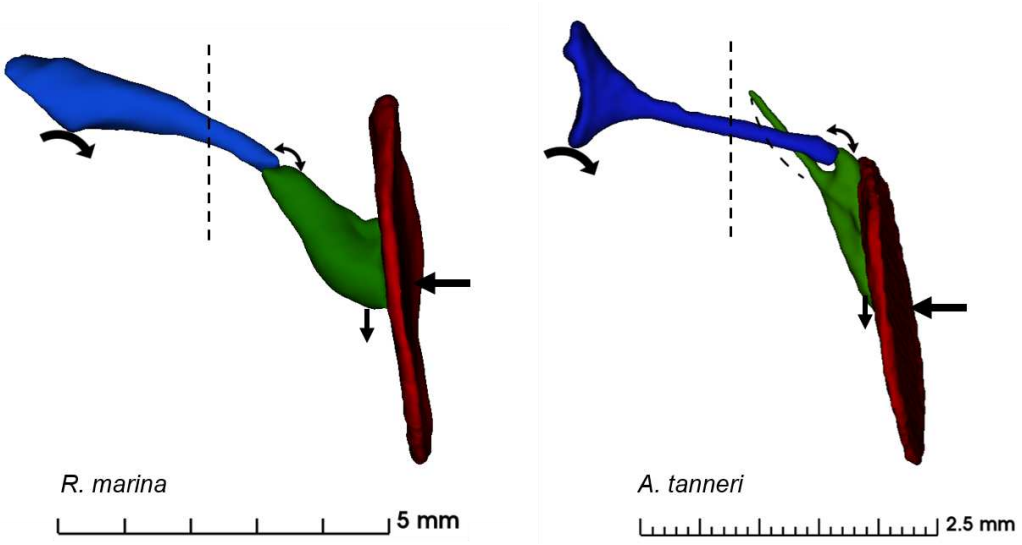

Figure 2.3: Expected movement for the middle ear FE models at low frequencies (below 3 kHz) showing the tympanum (red), extracolumella (green), and columella (blue). The tympanic annulus was omitted for clarity. The arrows depict (right to left): an inflection of the tympanum, downward motion of the extracolumella, a small hinge motion at the articulation between the ossicles, the hypothetical location of the axis of rotation based on calculations from Mason and Narins 2002, and rotation about the footplate axis. Left: Predicted movement for *R. marina* middle ear. Right: Predicted movement for the *A. tanneri* middle ear. The dashed curve indicates flexion of the ascending process.

In addition to the movement of the baseline models, I explored the movement of the middle ear when the extracolumella was assigned bone-like material properties. I also analyzed the effects of removing the elastic footplate support, and the effects of a stiff rather than sliding connection between the tympanum and extracolumella.

II. Methods

Finite element (FE) models of the middle ears of *Rhinella marina* and *Arthroleptis tanneri* were created from CT scans using methods described in Chapter 1. A combination of animations and velocity vector visualizations were used to analyze the movement of the models at a range of frequencies. Simulations were performed in SimScale (simscale.com).

III. Results

R. marina Middle Ear Model: Modes of Movement

The frequency-dependent vibration modes of the *R. marina* middle ear FE model were characterized. Chapter 1 shows that the footplate and tympanum displacement results from the model resembles the empirical data for this species. However, analysis of the FE animations reveal that the movement differs from that described for other anurans. Rather than one mode of movement, *three* different modes of movement were observed; these were classified as being "piston-like", in which the tympanum and footplate move together in the same direction, "lever-like", in which the footplate and tympanum move in opposite directions, or "rocking", in which the medial end of the columella rocks gently about a fulcrum that is slightly more distal than the footplate axis. Visual representations of these movements are provided in Figure 2.4. The *R. marina* FE model had piston-like motion between 100-1,800 Hz, lever-like motion between 1,800-3,100 Hz, and rocking motion between 3,100-10,000 Hz. It is important to note that the term "lever" in the context of this study refers to a movement other than that described by the pump-handle hypothesis: instead of the fulcrum being at the footplate axis, it is on the flexible extracolumella. Additionally, the "rocking" motion features a fulcrum point near the footplate axis, and this could be thought of as representing the pump-handle hypothesis.

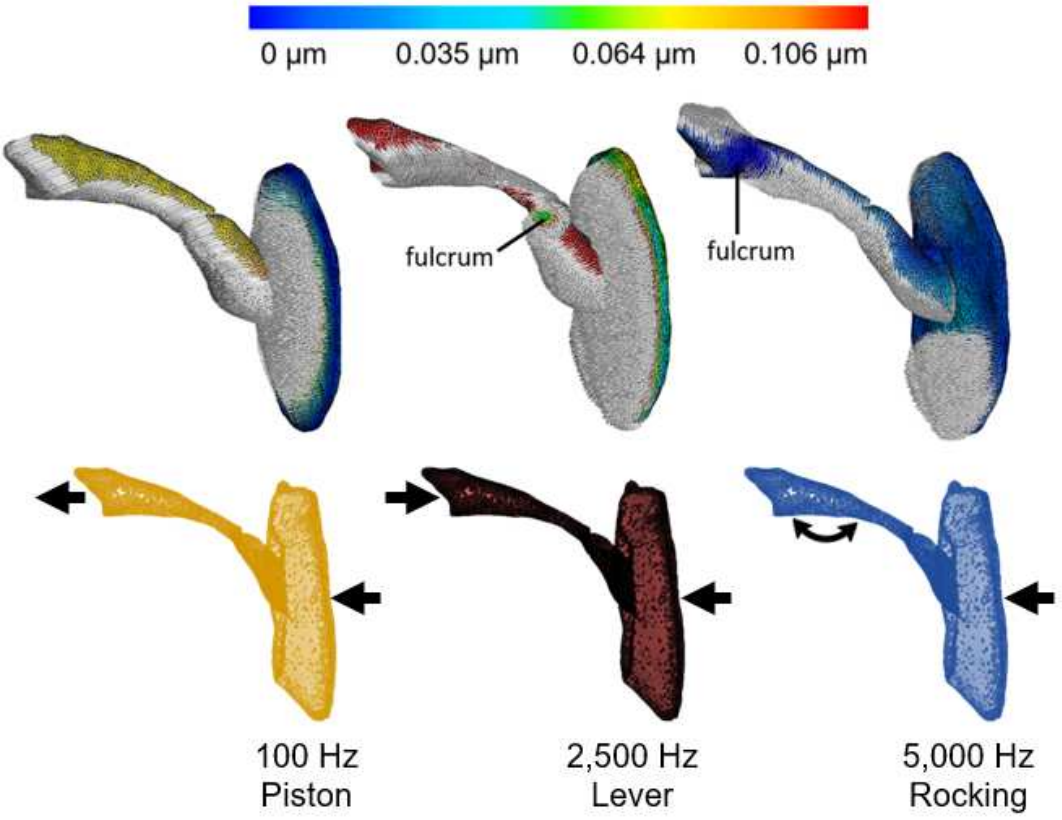

Figure 2.4: Top: Vector visualizations showing the magnitude of velocity in the *R. marina* middle ear model. The tympanic annulus was omitted for a more complete view. The color scale represents the magnitude of displacement for the models in the top row. The magnitude of the vectors is greatly exaggerated for clarity and their lengths are not relative. **Bottom:** Graphical representation of the movements depicted in the top row. The colors are coded to represent each mode in the following figures.

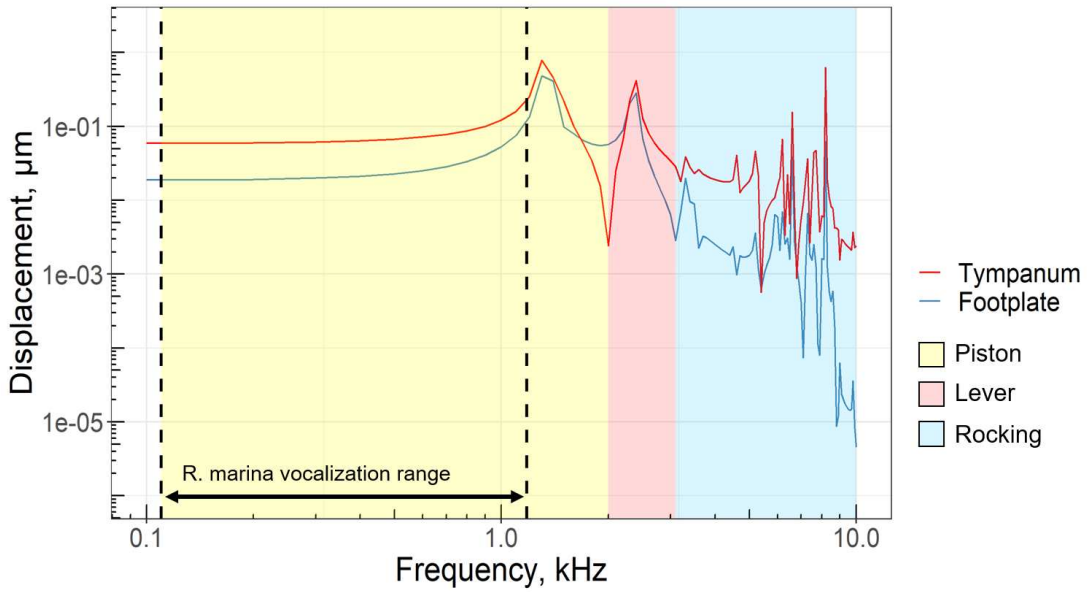

Figure 2.5: Baseline *R. marina* frequency response function. Background colors represent the range for different modes of movement observed in the FE model.

Characteristics of Movement

Inflection of the tympanum was observed for all frequencies. However, the pattern of displacement varies with frequency. The extracolumella was observed to slide downward by a small amount for most frequencies. There was a slight hinge-like movement between the columella and extracolumella in which the angle between these structures varies slightly. This was more during lever motion. A gentle rocking motion about the elastic support was observed in the animations, in which the footplate experiences forward and backward displacement. A summary of these characteristics is shown in Table 2.1.

Table 2.1: Summary of *R. marina* Movement Characteristics

Movement Characteristic	Observed?	Description
Tympanum inflection	Yes	Location of greatest displacement varies with frequency. High frequencies show complex displacement patterns.
Sliding of extracolumella down the tympanum	Yes	Amount of sliding depends on frequency. A significant amount of sliding is observed at 2-3 kHz, during lever-like motion. Sliding is in the downward direction for all frequencies except between 700-1200 Hz, in which an upward movement is observed.
Hinge-like articulation between extracolumella, columella	Yes	Slight decrease in angle for most frequencies, with the greatest change in angle occurring during lever-like motion (2-3 kHz).
Rotation about footplate axis	No	Little curvature or rotation observed at the footplate.

Sliding vs. Bonded Extracolumella

Mason and Narins 2002 described that the extracolumella moves downward upon inflection of the tympanum. To simulate these effects, a sliding contact was used between the tympanum and extracolumella. Animations revealed that sliding was in the downward direction upon inflection of the tympanum for frequencies other than 700-1200 Hz, in which an upward movement is observed. The amount of sliding was small for most frequencies. The most sliding is observed at 2-3 kHz, during lever-like motion. The results show that the nature of this contact does not play a major role in the overall movement of the model (Figure 2.6). The modes of movement with a fixed contact were observed for the same frequencies as when a sliding contact was used (baseline), and there is little difference in the magnitude of displacement. Instead of playing a major role in the mode of movement, the sliding appears to dampen the resonance

peaks. Based on the literature (Mason and Narins 2002), I suspect that real ears probably have greater amounts of sliding than predicted by the model, and this movement may still play a role in overall ear function. However, the results suggest that this feature may also have a secondary role in damping resonance peaks.

Effects of Elastic Footplate Support

Removal of the elastic footplate support results in there being little difference between tympanum and footplate displacement at low frequencies compared to the baseline model with an elastic footplate support with k=500 N/m (Figure 2.6). The presence of an elastic support with this spring constant decreases footplate motion at low frequencies by approximately 0.05 μm. The same three modes of movement occurred at the same frequencies as the baseline.

Cartilaginous vs. Bony Extracolumella

Amphibian ears, unlike those of mammals, have a cartilaginous ossicle: the extracolumella. To test the potential advantages of having this cartilaginous ossicle on ear movement, the extracolumella was assigned the same Young's modulus and density as the bony columella. The FE model predicts that having a stiff extracolumella prevents lever-like motion of the middle ear (Figure 2.6). The vector visualization at 2,500 Hz is shown in Figure 2.7. Instead, the model appears to shift from piston-like motion directly to rocking motion without a fulcrum on the extracolumella. However, the extracolumella may not need to be as stiff as bone in order to have this effect. To determine the stiffness at which the lever motion stops, I analyzed the motion of the FE animation at a range of Young's modulus values (not shown). I found that a Young's modulus of approximately 30 MPa or greater prevented flexion of the extracolumella and therefore lever-like movement.

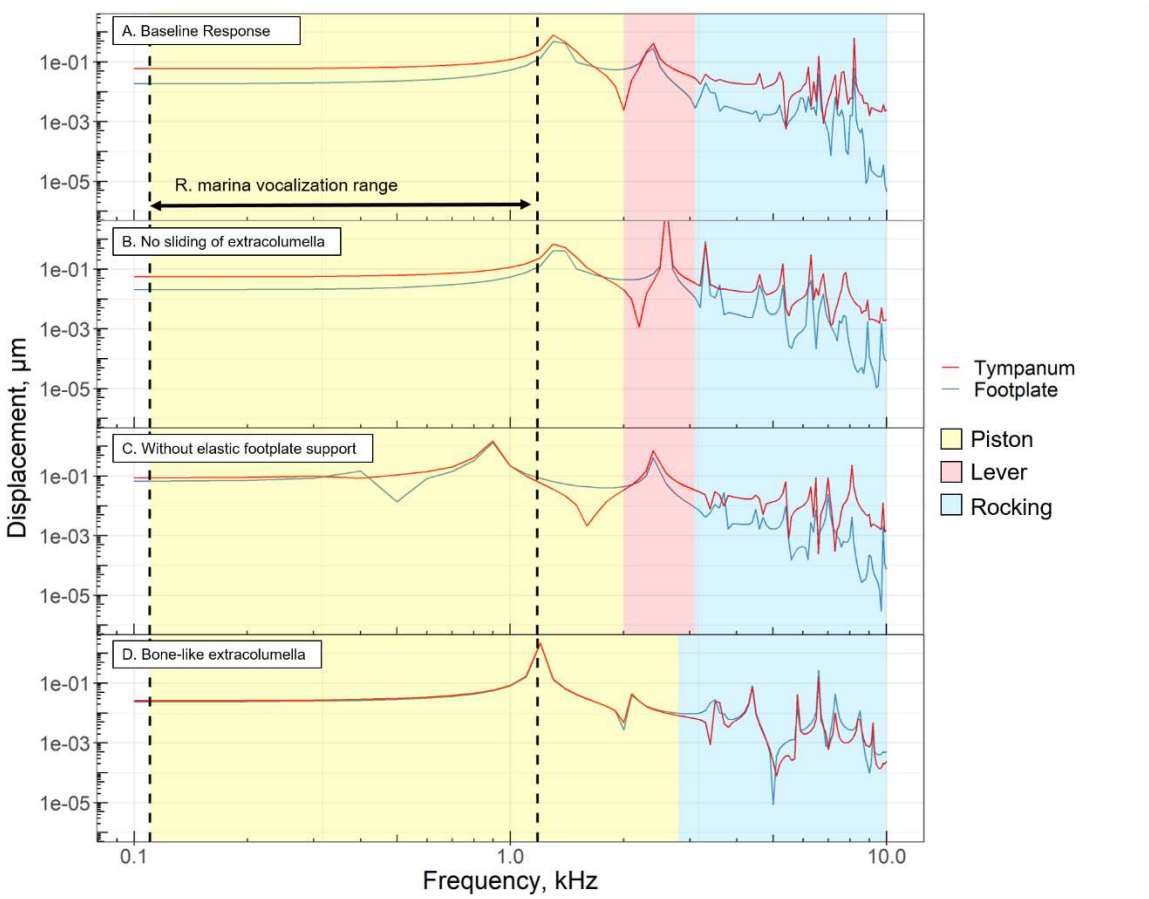

Figure 2.6: Summary of the results of varying parameters in the FE model of the *R. marina* middle ear. A. The baseline model in which no alterations were made. B. Effect of using a fixed support between the extracolumella and columella. C. The effect of removing the elastic footplate support that emulates the articulation between the ventral side of the footplate and the otic capsule. Note the small difference between the tympanum and footplate displacement at low frequencies. D. The effects of assigning bone-like material properties to the extracolumella, therefore reducing its flexibility. Note the absence of lever-like motion for this model.

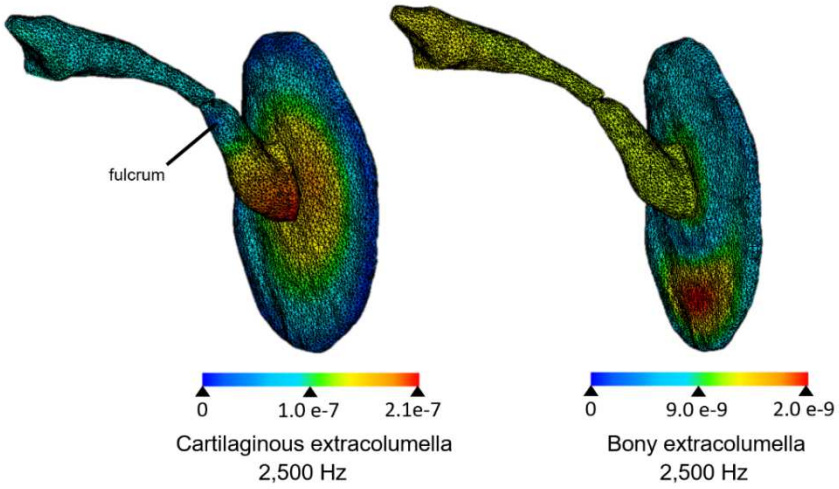

Figure 2.7: Effect of extracolumella material composition (cartilaginous vs. bony) on the mode of movement in the *R. marina* middle ear model at 2,500 Hz. The tympanic annulus was omitted for clarity. Note the lack of a fulcrum in the bony extracolumella model.

Model Limitations

Discrepancies in movement between the model and literature could be due to several factors. First, the model may be missing some features that are important for ear movement, which could prompt future studies of middle ear parameters that were not considered. Another reason could be that there are species differences in the modes of movement, and the ear of *R. marina* could function in a different way than that of Ranid frogs. A laser vibrometry study of the vibration of different *R. marina* ear components, similar to the study done in bullfrogs by Mason and Narins 2002, would elucidate whether or not the model behaves realistically. Furthermore, I did not observe an ascending process in the CT scan, but *R. marina* may typically have this structure. This model does not take into account the potential effects of the ascending process for this species. Lastly, the strength of the elastic support that mimics the attachment of the footplate to the oval window is not completely known. There was little to no visible rotation

observed about the footplate axis throughout the frequency range, which may indicate that the elastic support was not as rigid as in a real ear. Further studies on the nature of this connection would help inform this parameter.

A. tanneri Middle Ear Model: Modes of Movement

Characteristics of Movement

As with *R. marina*, inflection of the tympanum was observed for all frequencies, and the pattern of displacement varied with frequency (see "Effects of Frequency on Tympanum Vibration Pattern"). However, the extracolumella was not observed to slide at any frequencies. This may have been due to its relatively dorsal position on the tympanum and larger surface area in contact with the tympanum. There was a hinge-like motion between the columella and extracolumella in which the angle between these structures decreased as the tympanum pressed inward. The ascending process was mostly observed to compress and expand along its long axis, but there were a few select frequencies at which it was bending (e.g. 4-4.1 kHz). A gentle rocking motion about the elastic support was observed during piston-like movement. This is likely seen in *A. tanneri* but not *R. marina* due to the greater effect of the elastic support on a smaller ear. A summary of these characteristics is shown in Table 2.2.

Modes of Motion

The frequency-dependent vibration modes of the *A. tanneri* middle ear FE model were characterized as piston-like, lever-like, or rocking. Vector visualizations and a diagram for each mode of movement are shown in Figure 2.7. Despite differences in size and geometry, these

three modes were similar to those observed for *R. marina.* However, there were differences in the frequencies at which they occur, which are described in the next section.

Table 2.2: Summary of *A. tanneri* Movement Characteristics

Movement Characteristic	Observed?	Description
Tympanum inflection	Yes	Location of greatest displacement varies with frequency. High frequencies show more complex displacement patterns.
Sliding of extracolumella down the tympanum	No	Sliding was not observed at any frequency.
Bending of ascending process	Mostly No	Compression and expansion of the ascending process was observed for most frequencies. Bending was observed between 4-4.1 kHz and a few other frequencies.
Hinge-like articulation between extracolumella, columella	Yes	Decrease in angle for most frequencies.
Rotation about footplate axis	Yes	Rocking about this axis observed during piston-like motion.

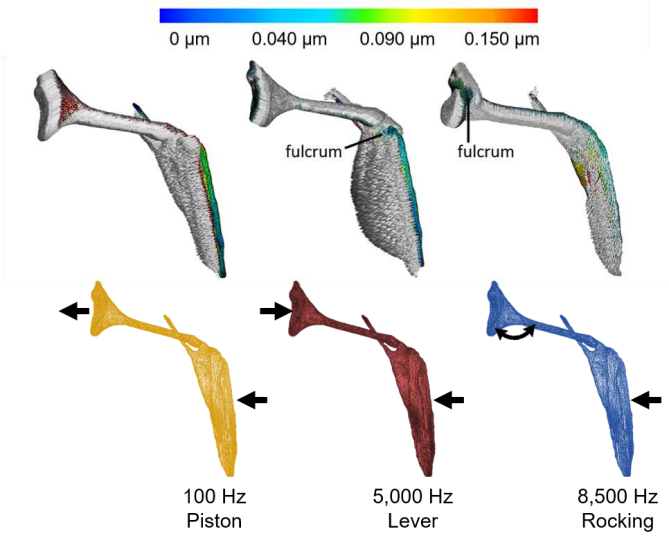

Figure 2.7: Vector visualizations showing the magnitude of velocity in the *A. tanneri* middle ear model. Tympanic annulus omitted for clarity.

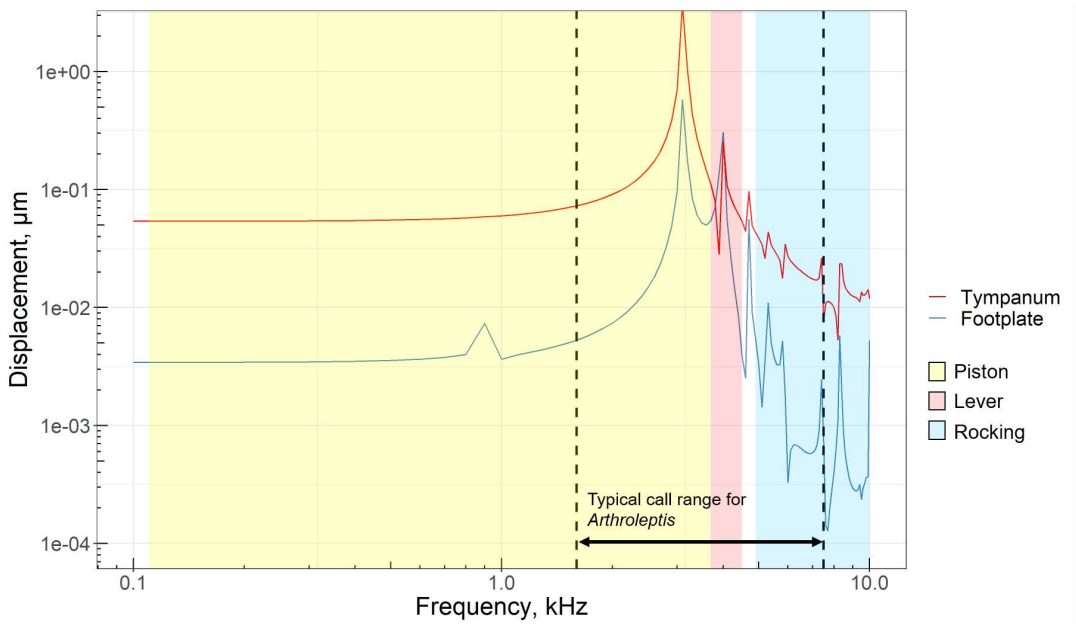

Figure 2.8: Baseline *A. tanneri* frequency response function. Background colors represent the range for different modes of movement observed in the FE model.

Modes of Motion: Species Comparison

Analysis of the FE model animations revealed that both models generally move in each of the three modes, but at different frequency ranges. Both middle ear models have piston-like motion at low frequencies. However, *R. marina* exhibits lever-like motion between 2-3 kHz, whereas in *A. tanneri* this motion occurs between 3.8-4.5 kHz. Both models then transition to rocking motion. This means that all three motions are present in the predicted calling range of *A. tanneri*, whereas piston-like movement dominates the calling range for *R. marina*. If this model accurately reflects the movements at this range of frequencies, it appears that there may not be an association between mode of movement and the vocalization range of the species. However, it is uncertain whether the movements produced by rocking contribute to hearing since the displacement drops off during this mode of movement. The baseline frequency response curve for *A. tanneri* is shown in Figure 2.8a. Since the tympanum began to vibrate at more complex

patterns at higher frequencies, assigning modes of the movement became difficult. The white space in the figure represents frequencies at which the movement was uncertain.

Sliding vs. Bonded Extracolumella

Assigning a bonded contact rather than a sliding contact to the extracolumella had little effect on the mode of movement at different frequencies (Figure 2.9b), and there was generally no significant difference in the amount of displacement, however, a sliding contact appears to have a slight damping effect on the resonance peaks. Another difference was that the region of uncertainty, where movement was uncharacterizable, became more narrow when a sliding contact was used.

Effects of Elastic Footplate Support

When an elastic footplate support was removed from the end of the columella, footplate displacement was much higher such that there was a much smaller difference in displacement between the tympanum and footplate (Figure 2.9c). Additionally, the footplate (but not tympanum) displacement dropped off far earlier, beginning at about 1 kHz, compared to when a support was present (beginning at about 5 kHz). This suggests that the articulation between the footplate and the otic capsule helps extend the range of frequencies transmitted to the inner ear.

Cartilaginous vs. Bony Extracolumella

Assigning bone-like material properties to the extracolumella produced interesting movement results (Figure 2.9d). Rather than pivoting on the footplate axis or extracolumella, the axis was located at various points along the columella. The location of the fulcrum along the

columella depended on the frequency. No bending of the extracolumella was observed, and the footplate did not move out of phase with the tympanum.

Fixed vs. Free Ascending Process

When the fixed support at the tip of the ascending process was removed, the model did not show a significant difference in behavior (Figure 2.9e). The only noticeable difference was a slight shift toward higher frequencies at which the model moved like a lever. Assuming the ascending process does play an important role in ear function, these results suggest that perhaps there are some parameters not present in the model that are important for proper functioning of the ascending process.

Comparison to R. marina at a Similar Size

To study the effect of size vs. geometry on model behavior, I compared the movement of *A. tanneri* to the movement of *R. marina* scaled by 0.5x to account for size differences (Figure 2.9f). The shape of the frequency response curve for the smaller *R. marina* ear is much more similar to that of *A. tanneri*. The modes of movement were also similar to those of *A. tanneri*, though the lever movement occurs at slightly higher frequencies in *R. marina*. Since the size and the spring constant of the elastic footplate support were the same, I was able to compare the difference between tympanum and footplate displacement. Even accounting for size, the difference is still far more pronounced for *A. tanneri* than *R. marina* throughout the entire frequency range, which suggests that this species is somehow more sensitive to the rigidity of this connection or lacks the vertical displacement needed to set the footplate axis rotation in motion. Overall, these results suggest that size plays a substantial role in the magnitude of displacement, shape of the frequency response curve, and mode of movement. However, there

may be differences in geometry that influence the displacement gap between the footplate and tympanum.

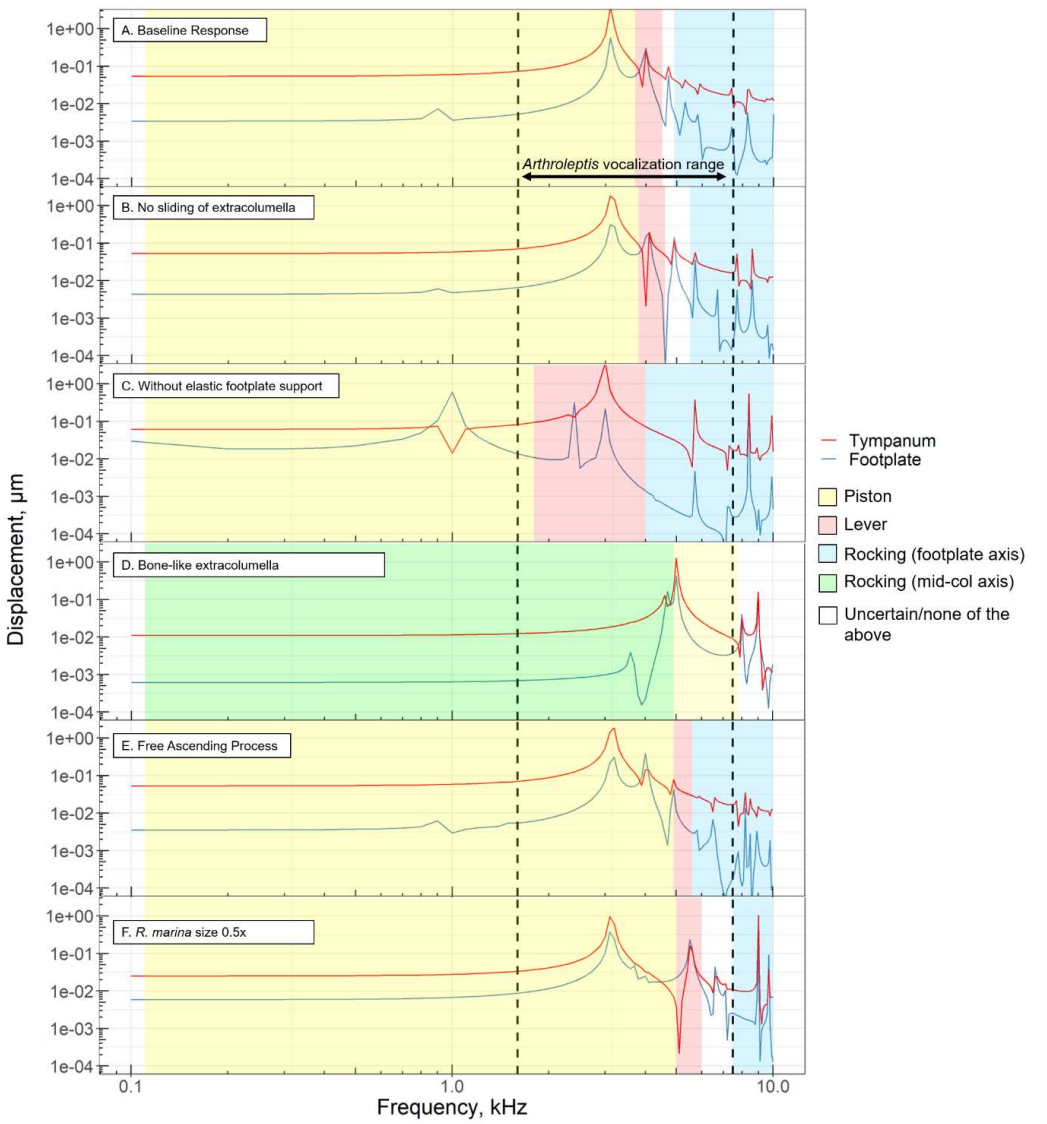

Figure 2.9: Summary of the results of varying parameters in the FE model of the *A. tanneri* middle ear, and of *R. marina* at about the same size (scaled 0.5x). A. Baseline response in which no alterations were made. B. Fixed support between the extracolumella and columella, C. Effect of removing the elastic footplate support that emulates the articulation between the ventral side of the footplate and the otic capsule. Note the small difference between the tympanum and footplate displacement at low frequencies. D. Effect of assigning bone-like material properties to the extracolumella, therefore reducing its flexibility. Note the absence of lever-like motion for this model and the relatively low displacement. E. Effect of a free ascending process, in which the fixed support was removed from the tip of this structure. F. Response of the *R. marina* model when scaled by a factor of 0.5 such that it is a similar size to the *A. tanneri* ear model.

Effects of Frequency on Tympanum Vibration Pattern

Interestingly, the footplate displacement becomes noisy at high frequencies for both ear models. When visualizing the movement at these frequencies, it was clear that the variation in movement was likely due to increasingly complex patterns of displacement on the tympanum. Visualizations of the relative displacements on the tympanum for each species are shown in Figure 2.10. At low frequencies, the pressure is neatly dispersed from the center of the tympanum outward, resulting in an even force pressing the extracolumella inward. At relatively high frequencies, the displacement pattern becomes more complex, which likely causes the extracolumella and columella to swing in various directions. This phenomenon complicates analysis at high frequencies. This effect is seen with the *R. marina* tympanum above 2 kHz and the *A. tanneri* tympanum at frequencies above approximately 6 kHz. There is a clear association between the simple, radiating pattern with piston-like movement and complex tympanum patterns with rocking motion. This difference in pattern between species is probably mostly due to size, since the *R. marina* tympanum is about twice as large. Visual inspection of the patterns in *R. marina* 0.5x showed that the range of even distribution was extended to 4 kHz (Figure 2.11). This provides further evidence that size is a main factor in the frequency-dependent behavior of the middle ear.

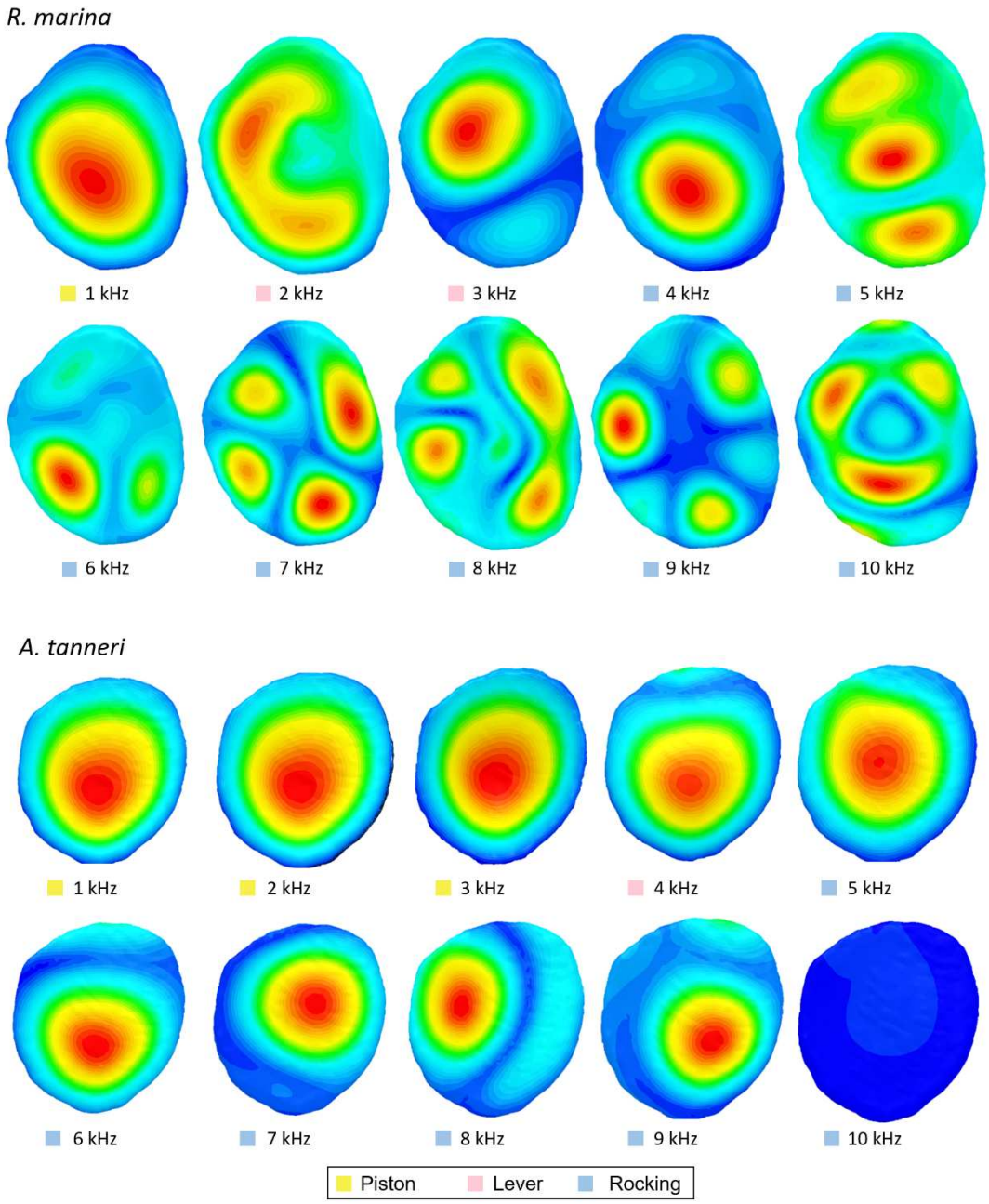

Figure 2.10: Lateral view of tympanums from both species. Colors depict the relative patterns of displacement throughout individual tympana, with red being the highest displacement and blue being the lowest displacement.

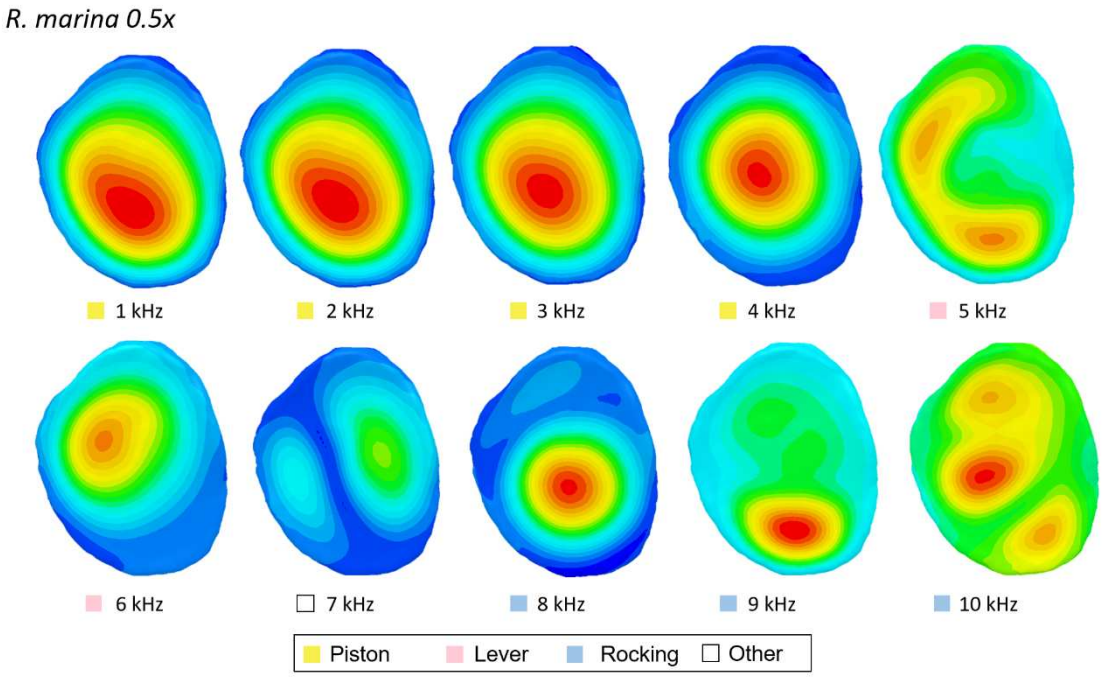

Figure 2.11: Lateral view of tympanums from *R. marina* scaled by 0.5x to approximately match the size of *A. tanneri*. Colors depict the relative patterns of displacement throughout individual tympana, with red being the highest displacement and blue being the lowest displacement.

I suspect that the reason for these patterns is mostly due to harmonic resonance, plus some influence from the attached mass from the rest of the middle ear. The patterns observed for the *R. marina* ear in particular are similar to those seen for Laguerre-Gaussian cylindrical transverse mode patterns (Figure 2.11), which may be an important factor for the limitations of hearing since displacement drops off significantly at frequencies at which these complex patterns occur. Since the middle ear essentially works as a broadband filter for sound frequencies, the size of the eardrum influences its response to a range of frequencies and essentially limits the sound frequencies that can be transmitted to the inner ear.

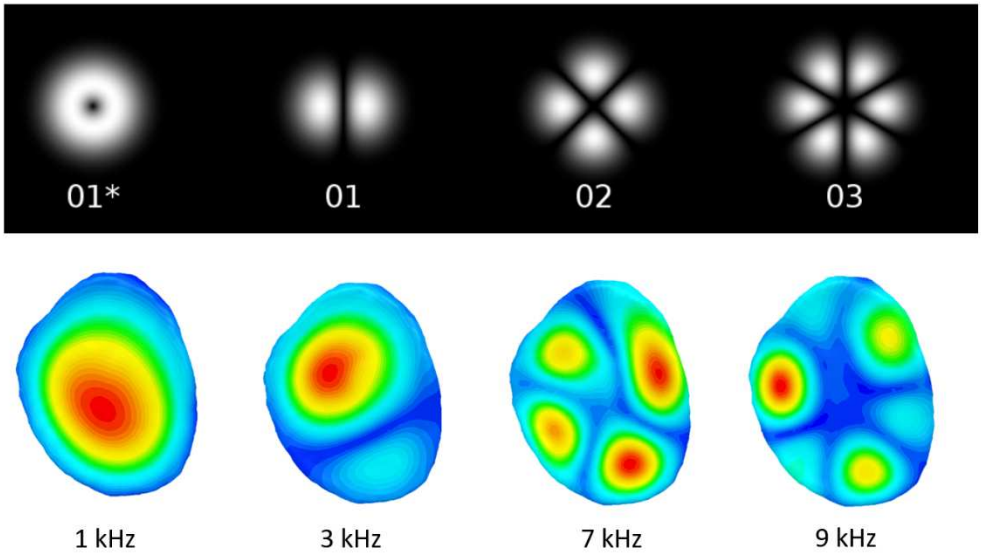

Figure 2.12: Top row: Laguerre-Gaussian transverse mode patterns (image credit: Wikimedia). Bottom row: representative tympanum patterns from *R. marina* that match each transverse mode pattern.

IV. Discussion

As previously mentioned, Mason and Narins (2002) predicted that the modes of ossicular vibration probably vary, especially at higher frequencies, and the position of the footplate axis may also change with frequency. This study supports their prediction by showing that there are three main modes of vibration for the baseline FE model, and that the position of the fulcrum in this predictive model is also frequency-dependent. Comparison of the two models give us reason to believe that something different is happening fundamentally between the ears of both species. However, the biological implications of these differences remain unclear, which can be used to set up future empirical work. It is also important to note that the models may be missing some important parameters. For example, as mentioned in the Chapter 1 discussion, there may be

important impacts from resonance of the eustachian tubes and mouth cavity. Future work on the effects of resonance on footplate displacement would help address this question.

Though the model matches what is known about anuran middle ear function in several ways, the models are not completely consistent with the literature. One point to consider here is that conclusions from empirical work using bullfrogs likely does not apply to all species of frogs. More empirical work in a broader range of species would help clarify the extent to which these characteristics are shared among anuran species. However, assuming the bullfrog ear accurately represents most frog ears, our results contradict empirical evidence that shows that the ascending process is crucial for proper ear functioning. Mason and Narins 2002 proposed that the ascending process bends to accommodate the downward movement of the extracolumella when the tympanum is inflected, and found that the middle ear of the bullfrog *Rana catesbiana* failed to transmit sound to the inner ear when the ascending process was severed. The model of *A. tanneri* predicts that the ascending process does not usually bend, even though it is flexible, and that ear function is relatively unaffected without this structure.

There are a few different explanations for this discrepancy. Although the study reported that the ear was not disturbed during the process, it may still be possible that the excision surgery interfered with the normal functioning of the ear. Alternatively, there may be some important features that the FE model does not capture. Mason and Narins found that the middle ear approaches the movement in Figure 2.2 C, in which the rotation is restricted to the articulation between the extracolumella and columella and results in very little displacement. I hypothesize that the ascending process aids in supporting this articulation, and that the models may represent this effect through their bonded contact at this position. Future work on the connection between these ear components may help inform our understanding of the role of the ascending process.

Additionally, not all frogs have an ascending process, and it would be interesting to study how their tympanic middle ear functions without this structure. As I mentioned in Chapter 1, no ascending process was observed while segmenting the *R. marina* CT scan. However, *R. marina* may typically have this structure. To test the effects of the ascending process, I have created an FE model of the *R. marina* middle ear with an artificial ascending process. These simulations are ongoing to determine the role of the ascending process in the movement and displacement.

Furthermore, size was shown to account for most of the species differences on the frequency response curve. However, controlling for size did not account for all of these differences. There is a much larger difference in displacement between the tympanum and footplate for *A. tanneri*, which reflects the impact of its geometry. Future research should analyze the effect of individual geometry components to determine which aspects of these features are most important for this difference. A summary of these differences in geometry is provided in Figure 1.8. The difference in geometry between the two species may offer separate advantages. One such advantage could be a higher mechanical advantage in the ear of *A. tanneri* during lever motion, since the fulcrum is closer to the load. This could be advantageous in amplifying sound pressure.

Another important topic for discussion is that the amount of displacement that reaches the inner ear does not necessarily equate with the ability to hear those frequencies. The middle ear acts as a broadband filter by selecting a subset of frequencies that vibrate the inner ear fluid. Inside the inner ear, the tectorial membrane and hair cells respond to fluid vibrations for further frequency selectivity (Schoffelen 2008). Given the variability in footplate movement seen in the model, it seems reasonable to wonder if the different modes of footplate movement impact inner

ear fluid vibration. Future work on this topic could offer important insights to how middle ear movement is translated by inner ear structures.

V. Summary and Conclusions

The main characteristics of motion were analyzed for each model. Downward sliding of the extracolumella was observed for *R. marina* but not for A. *tanneri*. There was hinge-like movement between the extracolumella and columella for both species. The model of *A. tanneri* showed rotation about the footplate axis during piston-like motion, but not the model of *R. marina*. The mode of movement is frequency-dependent: The *R. marina* ear model has piston-like movements between 0.1-2 kHz, lever motion between 2-3 kHz, and rocking motion between 3-10 kHz. The *A. tanneri* FE model has piston-like motion between 0.1-0.3 kHz, lever-like motion between 3-6.4 kHz, and rocking motion between 6.4-1kHz. The vocalization range for *R. marina* consists of piston-like movement, whereas the predicted range for *A. tanneri* exhibits all three types of movement. Removal of the elastic support increased footplate displacement at low frequencies in *A. tanneri*, but this displacement dropped off at much lower frequencies. In *R. marina*, the low frequency displacement was higher. Removing the effect of sliding did not appear to affect the behavior of either model, however, sliding appears to have a damping effect for both responses. Assigning bone-like material properties to the extracolumella prevented lever-like motion in both species and resulted in very low displacement in *A. tanneri*, but not *R. marina*. For both species, the tympana exhibited more complex displacement patterns with increasing frequency, and this was associated with a decrease in displacement. Overall, this study shows that the modes of movement in the frog middle ear may be frequency-dependent, and that differences in middle ear size and morphology can result in different vibratory behavior.

REFERENCES

Aernouts, J., Dirckx, J. J. **2012.** Viscoelastic properties of gerbil tympanic membrane at very low frequencies. *Journal of Biomechanics*, 45(6):919-24. doi: 10.1016/j.jbiomech.2012.01.023. Epub 2012 Feb 10. PMID: 22326125.

Beer, H. J., Bornitz, M., Hardtke, H. J., Schmidt, R., Hofmann, G., Vogel, U., Zahnert, T. and Hüttenbrink, K.B **1999**. Modelling of components of the human middle ear and simulation of their dynamic behaviour. *Audiology and Neurotology*, *4*(3-4), 156-162.

Bleach, I. T., Beckmann, C., Both, C., Brown, G. P., & Shine, R. **2015**. Noisy neighbours at the frog pond: effects of invasive cane toads on the calling behaviour of native Australian frogs. *Behavioral Ecology and Sociobiology*, *69*(4), 675-683.

Boistel, R., Aubin, T., Cloetens, P., Peyrin, F., Scotti, T., Herzog, P., Gerlach, J., Pollet,N. & Aubry, J. F. **2013**. How minute sooglossid frogs hear without a middle ear. Proceedings of the National Academy of Sciences, 110(38), 15360-15364.

Bolt, J. R., & Lombard, R.E. **1985**. Evolution of the amphibian tympanic ear and the origin of frogs. *Biological Journal of the Linnean Society*, *24*(1), 83-99.

Brown, G. P., Kelehear, C., Shilton, C. M., Phillips, B. L., & Shine, R. **2015**. Stress and immunity at the invasion front: a comparison across cane toad (Rhinella marina) populations. *Biological Journal of the Linnean Society*, *116*(4), 748-760.

Buser, T. J., Boyd, O. F., Cortés, Á., Donatelli, C. M., Kolmann, M. A., Luparell, J. L., Pfeiffenberger, J.A., Sidlauskas, B.L. & Summers, A. P. **2020**. The Natural Historian's Guide to the CT Galaxy: Step-by-Step Instructions for Preparing and Analyzing Computed Tomographic (CT) Data Using Cross-Platform, Open Access Software. *Integrative Organismal Biology*, *2*(1), obaa009.

Christensen-Dalsgaard, J., & Narins, P. M. **1993**. Sound and vibration sensitivity of VIIIth nerve fibers in the frogs Leptodactylus albilabris and Rana pipiens pipiens. *Journal of Comparative Physiology A*, *172*(6), 653-662.

Chung, S. H., Pettigrew, A. G., & Anson, M. **1981**. Hearing in the frog: dynamics of the middle ear. *Proceedings of the Royal Society of London. Series B. Biological Sciences*, *212*(1189), 459-485.

Cignoni, P., Callieri, M., Corsini, M., Dellepiane, M., Ganovelli, F., & Ranzuglia, G. **2008**. Meshlab: an open-source mesh processing tool. In *Eurographics Italian chapter conference* (Vol. 2008, pp. 129-136).

Elkhouri, N., Liu, H., & Funnell, W. R. J. **2006**. Low-frequency finite-element modeling of the gerbil middle ear. *Journal of the Association for Research in Otolaryngology*, *7*(4), 399-411.

Fedorov, A., Beichel, R., Kalpathy-Cramer, J., Finet, J., Fillion-Robin, J-C., Pujol, S., Bauer, C., Jennings, D., Fennessy, F.M., Sonka, M., Buatti, J., Aylward, S.R., Miller, J.V., Pieper, S., Kikinis, R. 3D Slicer as an Image Computing Platform for the Quantitative Imaging

Network. Magn Reson Imaging. 2012 Nov;30(9):1323-41. PMID: 22770690. PMCID: PMC3466397.

FreeCAD (Version 0.18) [Computer Software]. **2019**. Retrieved from https://www.freecadweb.org/.

Funnell, W. R. J., Maftoon, N., & Decraemer, W. F. **2012**. Mechanics and modelling for the middle ear. *Retrieved March*, *3*, 2013.

Hetherington, T. E., & Lindquist, E. D. **1999**. Lung-based hearing in an "earless" anuran amphibian. Journal of Comparative Physiology A, 184(4), 395-401.

Hoffstetter, M., Lugauer, F., Kundu, S., Wacker, S., Perea-Saveedra, H., Lenarz, T., Hoffstetter, P., Schreyer, A.G. and Wintermantel, E. **2011**. Middle ear of human and pig: a comparison of structures and mechanics.

Gan, R. Z., Feng, B., & Sun, Q. **2004**. Three-dimensional finite element modeling of human ear for sound transmission. *Annals of Biomedical Engineering*, *32*(6), 847–859. https://doi.org/10.1023/B:ABME.0000030260.22737.53

Grandison, A. G. **1983**. *A New Species of Arthrolepis (Anura: Ranidae) from the West Usambara Mountains, Tanzania*. British Museum (Natural History).

Hetherington, T. E. **1985**. Role of the opercularis muscle in seismic sensitivity in the bullfrog Rana catesbeiana. *Journal of Experimental Zoology*, *235*(1), 27-34.

Higashimachi, T., & Toriya, R. **2015**. Finite element analysis of the human middle ear and an application for clinics for tympanoplasty (Static and Harmonic Vibration Analysis). *American Transactions on Engineering & Applied Sciences*, *4*(1), 13-29.

Jaslow AP, Hetherington TE, Lombard RE . **1988**. Structure and function of the amphibian middle ear. In: Fritzsch B, Ryan MJ, Wilczynski W, Hetherington TE, Walkowiak W (eds) The evolution of the amphibian auditory system. Wiley, New York, pp 69-91

Jørgensen, M. B., & Kanneworff, M. **1997**. Middle ear transmission in the grass frog, Rana temporaria. *Journal of Comparative Physiology A*, *182*(1), 59-64.

Koike, T., Wada, H., & Kobayashi, T. **2002**. Modeling of the human middle ear using the finite-element method. *The Journal of the Acoustical Society of America*, *111*(3), 1306-1317.

Liu, Y., Higashimachi, T., & Toriya, R. **2019**. Numerical modelling and vibration analysis of human middle ear for application in sound conduction reconstruction. In IOP Conference Series: *Materials Science and Engineering* (Vol. 657, No. 1, p. 012037). IOP Publishing.

Maftoon, N., Funnell, W. R. J., Daniel, S. J., & Decraemer, W. F. **2015**. Finite-element modelling of the response of the gerbil middle ear to sound. *Journal of the Association for Research in Otolaryngology*, *16*(5), 547-567.

Manley, G. A. **1990**. The middle ear. In *Peripheral Hearing Mechanisms in Reptiles and Birds* (pp. 27-51). Springer, Berlin, Heidelberg.

Mason, M. J. **2007**. Pathways for sound transmission to the inner ear in amphibians. In *Hearing and sound communication in amphibians* (pp. 147-183). Springer, New York, NY.

Mason, M. J., & Farr, M. R. **2013**. Flexibility within the middle ears of vertebrates. *Journal of Laryngology & Otology*, *127*(01), 2-14.

Mason, M. J., & Narins, P. M. **2002**. Vibrometric studies of the middle ear of the bullfrog Rana catesbeiana II. The extrastapes. *Journal of Experimental Biology*, *205*(20), 3167-3176.

Mercurio, V. **2009**. Advertisement Calls of Three Species of Arthroleptis (Anura: Arthroleptidae) from Malawi. *Journal of Herpetology*, *43*(2), 345-350.

Meshmixer [Online]. **2017**. https://www.meshmixer.com/

Motallebzadeh, H., Maftoon, N., Pitaro, J., Funnell, W. R. J., & Daniel, S. J. **2017**. Finite-element modelling of the acoustic input admittance of the newborn ear canal and middle ear. *Journal of the Association for Research in Otolaryngology*, *18*(1), 25-48.

Narins, P. M., Ehret, G., & Tautz, J. **1988**. Accessory pathway for sound transfer in a neotropical frog. Proceedings of the National Academy of Sciences, 85(5), 1508-1512.

Nie, X., Liu, H., Huang, X., Tan, J., Xie, X., Yao, W., Rao, Z. and Duan, M. **2011**. Finite element model of human ear reconstruction through micro-computer tomography. *Acta oto-laryngologica*, *131*(3), 269-276.

O'Connor, K. N., Cai, H., & Puria, S. **2017**. The effects of varying tympanic-membrane material properties on human middle-ear sound transmission in a three-dimensional finite-element model. *The Journal of the Acoustical Society of America*, *142*(5), 2836-2853.

OnShape [Online]. **2014**. Retrieved from https://www.onshape.com/en/platform/.

Prendergast, P. J., Ferris, P., Rice, H. J., & Blayney, A. W. **1999**. Vibro-acoustic modelling of the outer and middle ear using the finite-element method. *Audiology and Neurotology*, *4*(3-4), 185-191.

Rolfe, S., Pieper, S., Porto, A., Diamond, K., Winchester, J., Shan, S., Kirveslahti H, Boyer D., Summers A., Maga, A. M. **2020**. *SlicerMorph: An open and extensible platform to retrieve, visualize and analyze 3D morphology.* BioRxiv, 2020.11.09.374926. https://doi.org/10.1101/2020.11.09.374926.

Saunders, J. C., & Johnstone, B. M. **1972**. A comparative analysis of middle-ear function in non-mammalian vertebrates. *Acta oto-laryngologica*, *73*(2-6), 353-361.

Schoffelen, R. L., Segenhout, J. M., & Van Dijk, P. **2008**. Mechanics of the exceptional anuran ear. Journal of Comparative Physiology A, 194(5), 417-428.

Smotherman, M. S., & Narins, P. M. **2000**. Hair cells, hearing and hopping: a field guide to hair cell physiology in the frog. *Journal of Experimental Biology*, *203*(15), 2237-2246.

Smotherman, M.S. & Narins, P. M. **2004**. Evolution of the amphibian ear. In *Evolution of the vertebrate auditory system* (pp. 164-199). Springer, New York, NY.

Sun, Q., Gan, R. Z., Chang, K. H., & Dormer, K. J. **2002**. Computer-integrated finite element modeling of human middle ear. *Biomechanics and modeling in mechanobiology*, *1*(2), 109-122.

"SimScale". **2019**. SimScale.com, [Online]. Available: https://www.simscale.com

Van Dijk, P., Mason, M. J., Schoffelen, R. L., Narins, P. M., & Meenderink, S. W. **2011**. Mechanics of the frog ear. *Hearing research*, *273*(1-2), 46-58.

Wada, H., Metoki, T., & Kobayashi, T. **1992**. Analysis of dynamic behavior of human middle ear using a finite‐element method. *The Journal of the Acoustical Society of America*, *92*(6), 3157-3168.

Wang, X. & Gan, R. Z. **2016**. 3D finite element model of the chinchilla ear for characterizing middle ear functions. *Biomechanics and modeling in mechanobiology*, *15*(5), 1263-1277.

Wang, X., Hu, Y., Wang, Z., & Shi, H. **2011**. Finite element analysis of the coupling between ossicular chain and mass loading for evaluation of implantable hearing device. *Hearing research*, *280*(1-2), 48-57.

Werner, Y. L. **2003**. Mechanical leverage in the middle ear of the American bullfrog, Rana catesbeiana. *Hearing research*, *175*(1-2), 54-65.

Wever, E. G. **1985**. *The amphibian ear*. Princeton University Press.